Composite Structures 373 (2025) 119678

Contents lists available at ScienceDirect

Composite Structures

journal homepage: www.elsevier.com/locate/compstruct

Manufacture, process simulation, modelling and testing of thick-walled thermoset fibre-polymer composite laminates — A review☆

Richard Protz [a],*, Eckart Kunze [a], Tim Luplow [b], Linus Littner [c], Jonas Drummer [d], Sebastian Heimbs [b], Marc Kreutzbruck [c], Bodo Fiedler [d], Maik Gude [a]

[a] TUD Dresden University of Technology, Institute of Lightweight Engineering and Polymer Technology (ILK), Holbeinstr. 3, 01307 Dresden, Germany
[b] Technische Universität Braunschweig, Institute of Aircraft Design and Lightweight Structures (IFL), Hermann-Blenk-Str. 35, 38108 Braunschweig, Germany
[c] University of Stuttgart, Institut für Kunststofftechnik (IKT), Pfaffenwaldring 32, 70569 Stuttgart, Germany
[d] Hamburg University of Technology, Institute of Polymers and Composites, Denickestraße 15, 21073 Hamburg, Germany

ARTICLE INFO

Keywords:
Thick-walled composites
Modelling
Process simulation
Manufacturing
Testing
Non-destructive testing

ABSTRACT

Thick-walled thermoset fibre-reinforced polymer (FRP) composites present unique challenges across their manufacturing, simulation, modelling, and testing processes. This paper provides a comprehensive overview of the current challenges and research needs associated with thick-walled FRP, particularly in light of their growing relevance in demanding application domains, such as wind energy. It is important to emphasise that the designation of a laminate as thick-walled is determined not solely by its nominal thickness, but also by the direction of the applied load. In particular, laminates subjected to compressive loading are typically considered thick-walled from a wall thickness of 4 mm or greater. While conventional manufacturing techniques remain applicable to thick-walled FRPs, process adaptations, such as adjusted curing cycles or alternative curing methods, are necessary to mitigate manufacturing defects, e.g. residual stresses induced by inhomogeneous curing due to local temperature overshoot. Modelling of the curing process and accurate prediction of residual stress development remain key areas of ongoing research with significant gaps in understanding. The influence of the wall thickness can also be seen in quasi-static and impact tests. Self-heating must be taken into account in fatigue tests and must be incorporated into future guidelines for the design of thick-walled FRP structures. While well-established non-destructive testing (NDT) techniques are generally applicable, their effectiveness is reduced with increasing laminate thickness due to limitations in resolution. The findings underscore the need for continued interdisciplinary efforts to refine processing and evaluation methods for thick-walled FRP composites.

1. Introduction

Thick-walled fibre reinforced polymer composites (FRP) are required to transfer extreme mechanical loads in structural components [1]. As Fig. 1 shows, they have already been established for years for load-bearing structural components in aircraft construction [2,3], rotor blades for wind turbines [4–7], pressure vessels [8,9], cryogen tanks [10–12], marine structures [13–15], leaf springs for light duty commercial vehicles [16], civil infrastructure [17,18] and tubes for offshore applications [19–21]. In particular, efforts to install wind turbines with a higher-rated output are leading to turbines with longer composite blades. In order to guarantee their load-bearing capacity, the wall thicknesses of the rotor blades must also be increased.

As laminate thickness increases, so do the challenges of manufacturing, non-destructive and destructive testing. While the difficulty in manufacturing is to ensure production quality at the level of thin-walled laminates, the effort in the construction and design of thick-walled FRP is to account for possible reductions in mechanical properties such as compression strength [22,23], and tension and bending strength [24]. Until now, this influence has not been taken into account in many manufacturing guidelines and test standards and therefore must be included in the form of safety factors. This reduces the potential for lightweight construction. In addition, the minimum wall thickness above which FRP laminates are labelled as thick-walled is not always consistent in the literature and seems to depend on the perspective, whether its from a geometric, structural mechanics, material testing, or manufacturing point of view. For example, Balvers et al. defines in [25] thick-walled structures from 10 mm upwards,

☆ This article is part of a Special issue entitled: 'Rolfes 65th' published in Composite Structures.

* Corresponding author.
E-mail address: richard.protz@tu-dresden.de (R. Protz).

https://doi.org/10.1016/j.compstruct.2025.119678
Received 3 April 2025; Received in revised form 22 August 2025; Accepted 16 September 2025
Available online 22 September 2025
0263-8223/© 2025 The Authors. Published by Elsevier Ltd. This is an open access article under the CC BY license (http://creativecommons.org/licenses/by/4.0/).

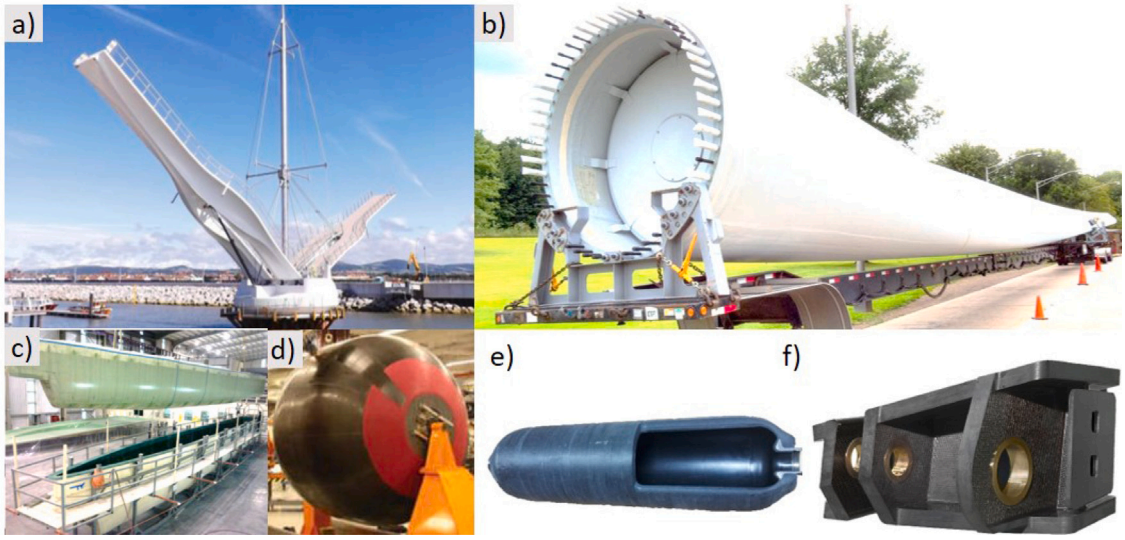

Fig. 1. Selected examples of thick-walled FRP components, (a) liftable FRP-footbridge [18], (b) wind turbine blade of recycled glass fibre [7], (c) side wall of a marine composite structure [15], (d) cryotank [10], (e) hydraulic bladder accumulator, and (f) aircraft main landing gear attachment [2].

whereas Nsengiyumva et al. in [26] from 15 mm upwards. From a structural mechanics point of view Kim et al. defines a box section beam with a wall-thickness t to profile height ratio >0.1 as thick-walled [27]. Laminates under quasi-static compressive load are characterised as thick-walled from a wall thickness of 4 mm [22,28] and under tensile load from a wall thickness of 10 mm [29,30]. Regarding manufacturing-related effects, a necessary deviation from the manufacturer recommended cure cycle, which usually applies to thin laminates [25], seems a simple option, as exothermic reaction affects laminate quality in several ways. The cure cycle parameters provided in the datasheets of polymeric composite laminates are optimised for thin laminates, with $t < 5$ mm [31,32]. Furthermore, experts also categorise so-called ultra-thick laminates, whereby the laminate thickness required for this is specified differently. According to Esposito [33], this classification is already met at a wall thickness of 30 mm, whereas Nie et al. refers to 60 mm [34], Gao et al. 70 mm [23] and Rivard et al. describes laminates exceeding 100 mm as ultra-thick [35], e.g. in the root area of a wind turbine blades. A universally accepted threshold for defining thick-walled laminates is not established in the literature. Bogetti et al. suggests a modified Damköhler number to define an analytical solution for a critical thickness, below which the exothermic temperature rise during curing remains limited and controllable under symmetric thermal boundary conditions imposed by isothermal tooling [36]. This critical Damköhler number depends on the temperature boundary conditions and cure kinetics only and provides manufacturers with a first threshold thickness. This is a first step taking manufacturing boundary conditions into account for a more precise classification, additionally the loading conditions should be considered. This article therefore provides a comprehensive overview of the special aspects and challenges involved in the manufacture and characterisation of thick-walled FRP laminates.

2. Manufacture, process simulation and quality control of thick-walled FRP

Thick-walled FRP laminates present significant challenges in both production and quality control. These challenges can give rise to so-called thickness effects, which are generally categorised into statistical and technological size effects. The statistical size effect is attributed to the increased probability of defects occurring within a larger stressed volume, which leads to a reduction in observed strength compared to smaller volumes. The technological size effect arises from process-related differences between the manufacturing of thick-walled and thin-walled FRP laminates [37]. In thick-walled thermoset matrix laminates, thickness-related effects can emerge during fibre placement, impregnation, and curing. These effects may manifest as fibre misalignments (both in-plane and out-of-plane), wrinkling, and resin-rich areas within or between filament bundles (rovings) [38,39], often resulting from insufficient compaction. Additionally, residual stresses and spring-back effects caused by uneven curing are more pronounced in thicker laminates, with all these phenomena strongly dependent on laminate thickness [37,40]. In thick FRP laminates, these manufacturing defects can develop locally but also globally and lead to varying mechanical properties [22]. Whether the effects are considered manufacturing defects depends on the number, location and size of the local stiffness and strength reserves of the component, as well as the application sector [40]. In the aerospace industry, the permissible limits are very narrow, while in the automotive industry a compromise must be found between manufacturing effects and process stability in favour of short cycle times.

2.1. Manufacturing process

Based on fibre placement and impregnation with a thermoset matrix, the established FRP manufacturing processes can be divided into the following three groups, particularly for the production of thick-walled laminates:

- The first group includes processes in which the fibres are deposited dry with subsequent fibre impregnation using liquid composite moulding processes. Curing takes place after complete fibre impregnation (Fig. 2a,c).
- The second group includes processes in which pre-impregnated or wet fibres are laid down on a mould. Curing takes place after the fibre lay-up has been completed (Fig. 2b).
- The third group includes processes in which the sequence or process steps of fibre placement and fibre impregnation cannot be clearly seperated, as in pultrusion (Fig. 2d).

The final step in all processes is curing. Regardless of the manufacturing process, the curing of thick-walled laminates is problematic because of the exotherm-generated heating during the chemical reaction. Subjecting thick laminates to the curing cycle recommended by the manufacturer, that is usually designed for thin-walled laminates, can lead to manufacturing defects [41,42]. Due to the large laminate thickness and low thermal conductivity of the composite, the heat of

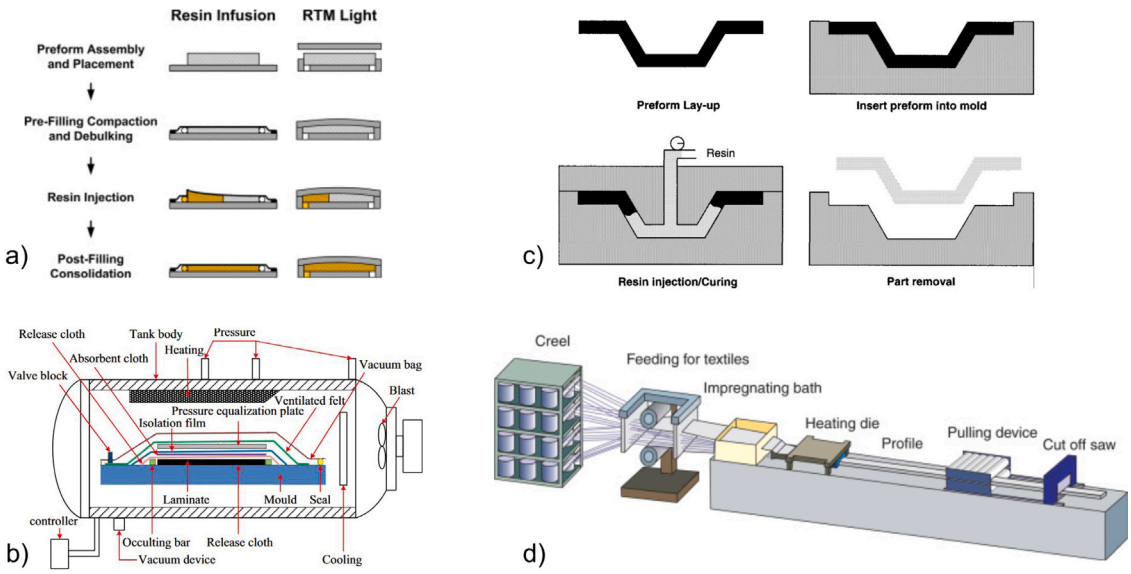

Fig. 2. Selected manufacturing processes for thick-walled composites: processes with flexible tooling (a) VARI, VAP and Light-RTM [52], (b) autoclave process [53], (c) process with rigid tooling (RTM) [54], (d) pultrusion process [55].

the reaction can be poorly dissipated, leading to laminate overheating and sometimes thermal damage when the degradation temperature is exceeded. To prevent this, the curing temperature must be lowered; otherwise the component can only be produced in layers step by step [34]. Both measures increase the production time. In order to prevent laminate damage due to exothermic temperature peaks and reduced heat dissipation, the temperature can be increased in stages until the maximum curing temperature is reached [43,44]. Another approach is the numerical optimisation of the curing cycles; see Section 2.2. Other approaches to prevent temperature overshoot in thick composites are layerwise curing [45], the use of different accelerator concentrations in the outer and inner sections of ultra thick laminates [46] and controlled layered self-resistance electric heating [47]. Microwave curing is proposed by Thostenson et al. in [48], as it provides instantaneous and controllable heat generation (compared to conventional oven curing) from the inside to the outside. The elimination of the thermal lag results in better control over the spatial solidification within the composite laminate, resulting in only minor matrix cracks in the end product due to residual stresses [49]. Nsengiyumva et al. gives a brief overview of material processing flaws and composite manufacturing defects that also apply to thick composite, stating that uneven temperature across the laminate thickness results in temperature gradients [26]. In prepreg-autoclave processing, these temperature gradients lead to uneven compaction, because the temperature dependant viscosity does not change homogeneously across the part in pre-impregnated laminates. Void formation [43] and differences in fibre volume fraction across the laminate thickness [41] are a consequence of inhomogeneous compaction. Furthermore, a temperature gradient results in uneven cure leading to residual stressses [50,51] or warpage [37]. In the worst case, residual stresses lead to delamination [29]. Residual stresses can also occur during cooling to room temperature at the end of the curing cycle due to anisotropic coefficients of thermal expansion [41].

The main challenges in manufacturing thick composites are thus related to fibre compaction, resin flow and curing and can be summarised as follows:

- **Nesting effects during fibre bed compaction**, including geometrical distortions, inter-tow gaps, and variations in internal structure, lead to locally varying permeability and fibre volume content [56–58].
- **Locally varying permeability** results in inhomogeneous flow fronts, increasing the risk of dry spot and void formation [59].
- **Delayed heating at the laminate core** in thick prepreg parts, caused by the low thermal conductivity of composites, postpones viscosity reduction and hinders adequate fibre compaction; this promotes an outside-in curing progression [60,61].
- **Temperature overshoots** due to the resin's exothermic reaction and low thermal conductivity lead to internal heat buildup, which can cause excessive temperatures and potential matrix degradation [49,62–64].
- **Non-uniform temperature and degree-of-cure profiles** across the laminate thickness arise from poor thermal conductivity [63].
- **Cure gradients through the thickness** result in incomplete fibre compaction, which leads to void formation, residual stresses, and matrix cracking; part warpage occurs as a consequence of these residual stresses [61,64].

2.1.1. Deposition of dry fibres in combination with liquid composite moulding processes

When processing dry fibres, the reinforcing material to be inserted into the cavity prior to infiltration is usually produced in an upstream preforming process. For components, woven or non-woven fabrics are cut to size, formed into a preform and the shape fixed using powder binder technology. Fibre deformations from the forming of semi-finished textile products are discussed in [65,66]. For hollow structures, such as drive shafts, braiding technology, or dry winding are often used as efficient direct preforming processes, Fig. 3.

Using braiding technology, reinforcing fibres such as carbon fibres and glass fibres can be dry laid onto the mandrel at very high speed [67]. The fibre orientation in braided structures can be tailored along the component axis to align with local stress distributions [68]. However, fibre waviness in the thickness direction poses a problem during dry fibre deposition [69]. In conventional braiding, two main effects are observed: first, the interlacing of rovings, leading to laminate densification. This mitigates resin-rich zones at crossover points, but increases out-of-plane undulations that are similar to those in woven fabrics and which degrade the mechanical properties. Second, fibre nesting, defined as the local interpenetration or shifting of adjacent layers, alters permeability, compaction, and resin flow. Nesting typically results in a total preform thickness smaller than the sum of the individual layers, thereby influencing the local permeability, e.g. in edge and corner areas. A braiding process is described by Gardiner et al. in which a uniaxial braid of reinforcing rovings and support yarns (like

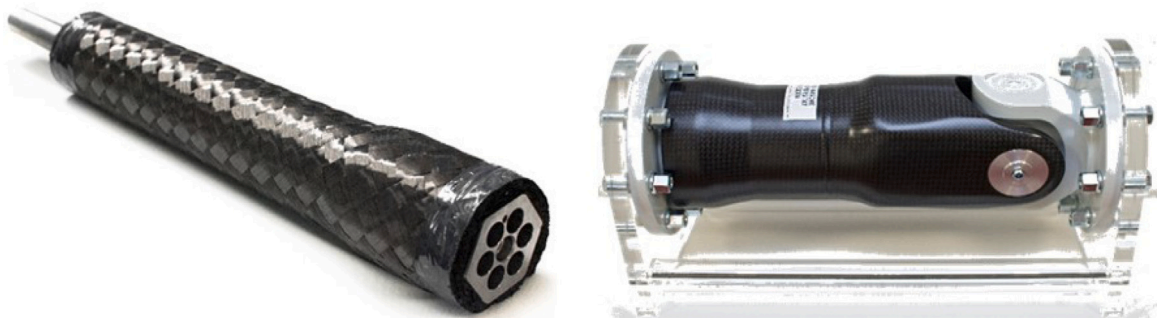

Fig. 3. Thick-walled braided and RTM-infiltrated drive shaft (left) and drive shaft with integrated cardan joint fork (right).

a unidirectional fabric) is laid on the core and undulation is almost completely avoided [70]. With the latter process, nesting can hardly occur. The preform is then placed with the core in the infiltration mould, impregnated, and consolidated. After or during demoulding the part, the core is removed. The liquid composite moulding (LCM) processes for impregnating dry preforms can be categorised into the following subprocesses established for the production of thick-walled laminates:

- Processes with a solid one-sided mould in combination with a flexible membrane,
- Processes with two closed rigid mould halves.

Typical processes using a flexible second mould half, usually a vacuum bag are VARI (vacuum assisted resin infusion) [34,71,72], the VAP process (vacuum assisted process) [73], which uses a semi-permeable membrane, and so called Light-RTM (resin transfer moulding) where the second mould half is usually a lamineted shell. Mould flexural stiffness plays a crucial role in regard to process consistency, because it affects resin pressure, cavity thickness and process time [52]. In LCM the driving force for resin impregnation is, according to Darcy's law, a pressure difference, thus the pressure in the impregnated fibres is always higher than in the dry fibres in front of the flow-front. This means, with flexible tooling, there is always an increase in laminate thickness in impregnated areas. After complete impregnation the inlet is closed and post filling thickness equilibration takes places in combination with excess resin bleed in the VARI process. In a VAP process, resin flow needs to be stopped after the correct amount of resin has entered the laminate, as the VAP membrane has no bleed port. Post filling thickness equilibration takes time in which the resin viscosity must be sufficiently low to allow for laminate compaction and equilibration. When curing starts during this phase thickness and thus fibre volume content variability occur. In the context of manufacturing components with substantial wall thickness through the VAP process, a methodology involving infiltrations conducted in two or more stages has been proposed by [34]. The outer section of the first laminate is precured and used as an outer tooling for the subsequent laminate sections. In summary, the utilisation of flexible tooling leads to greater thickness variation. Mould stiffness affects post-filling time significantly with more rigid moulds leading to shorter cycles as well as more consistent filling and eliminating thickness variability [52].

For processes with rigid closed moulds, a further distinction can be made according to the dispensing process: just using vacuum for the resin transfer, e.g. VARTM (vacuum assisted resin transfer moulding) [35], low-pressure processes, e.g. RTM using a pressure pot or low-pressure metering system [51,71] or high-pressure RTM (HP-RTM) [74,75] using a high-pressure metering machine. In processes using stiff moulds, fibre compaction occurs during mould closure and is therefore decoupled from the infiltration phase, resulting in a permeability dependant on the inital compaction state. This typically leads to lower permeability, resulting in more flow resistance and higher resin injection pressure. An alternative approach is offered by Compression Resin Transfer Moulding (C-RTM) [76], in which the mould remains partially open during the initial filling stage, allowing impregnation to occur under lower compaction. In C-RTM, the fibre preform is placed in the mould with a defined gap — typically between 0.5 and 2 mm — between the mould surface and the fibre stack [77,78]. This setup results in reduced flow resistance and higher permeability during form filling, often assisted by a metering system. Complete impregnation and final fibre compaction are achieved during a short, controlled closing stroke at the end of the injection phase, enabling efficient resin infiltration in the thickness direction.

In the low-pressure resin transfer moulding (RTM) process, impregnation of the fibre preform must be completed before a significant increase in resin viscosity occurs. This process can be operated either under constant pressure, using pre-mixed resin in a pressure pot, or under constant flow, using a low-pressure metering pump in combination with static mixers. To achieve full impregnation, it is generally necessary to employ resins with slow curing kinetics. Alternatively, if the resin exhibits a sufficiently broad range of acceptable viscosity, impregnation can also be facilitated by lowering the mould temperature. This leads to long process times, especially for thick laminates. For these reasons, the pressure pot RTM process is only used for very small to small batch production (lower then 10,000 units / year). For production volumes well above this number, constant-flow, low-pressure metering pumps are typically employed. In constant flow injection, the injection pressure must increase in order to maintain a constant flow rate. As the pressure within the mould cavity rises, the capacity of these pumps to compensate for the increased pressure is limited. This limitation alters the delivered flow rate, which may cause deviations in the mixing ratio and result in fluctuations in the overall process parameters. As a consequence, production repeatability is no longer guaranteed. High-pressure resin transfer moulding (RTM), based on the countercurrent mixing principle, addresses the limitations of constant flow, low-pressure RTM by providing a constant flow discharge and a substantially higher maximum flow rate, thereby reducing cycle time and enabling large-scale production of structural components. Both, epoxy and polyurethane resins with a very short pot life can be processed. Fast-curing resin systems with viscosities below 100 mPa s enable rapid infiltration of even thick-walled FRP structures with a high number of individual layers [75]. However, stiff tooling is a critical prerequisite for HP-RTM. When resin is injected at high discharge rates, fibre displacement may occur during mould filling—an effect that is more pronounced in thick-walled preforms compared to thin-walled ones. Additional manufacturing-related effects associated with liquid impregnation processes of thick-wlled FRP are summarised in [65]. Fully flexible moulds (Resin Infusion) are better suited for lower-cost, lower-precision applications but require longer post-filling times [52]. According to Barcena et al. the influence of the different LCM process variants with rigid tools on the formation of manufacturing defects can be summarised as follows [79]:

- Low pressure RTM minimises preform washout and micro-voids but exhibits high degree-of-cure variations.

- C-RTM balances cure uniformity but increases washout and voids.
- HP-RTM optimises cure consistency but maximises washout and micro-void formation.

The influence of different filling strategies for LCM processes is discussed in [52,79], statinng that convergent filling (peripheral inlet) is faster and consitently enhances dimensional stability of the cured parts, while divergent filling (one central inlet) leads to the greater geometric deviations in the final part. Taddei et al. had summarised mitigation strategies of infusion and cure-induced defects for thick composites especially produced with LCM processes [80]. Besides developing new thermosetting materials with low exotherm reactions, modelling process and material variability and using numerical simulations based on machine learning were identified as possible areas for future research.

2.1.2. Depositing pre-impregnated or wet fibres

This group includes manufacturing processes in which pre-impregnated fibres (prepregs) or wet fibres are placed in a mould and subsequently cured at room temperature or in an oven, possibly under pressure. Thick-walled laminates are produced by hand lay-up [43], wet winding [43,81–83], the prepreg autoclave process [29,44,84] and sheet moulding compound (SMC) pressing [85]. Despite the low achievable fibre volume content of 20% to 35%, hand lay-up and fibre spraying are still very widespread processes, e.g. for manufacturing of thick-walled laminates for tanks or flange connections. Here, layer thicknesses of a maximum of 12 mm to 15 mm are produced in a single pass. After a dwell time and the decay of the exothermic reaction peak, the laminating process can be continued. Another effect, especially with thick components, is the risk of sink marks due to resin shrinkage [43].

The prepreg autoclave process is a well-established production method, associated with excellent laminate quality in terms of high fibre volume content and low porosity [86]. Olivier et al. [41] and Twardowski et al. [42] describes the production of laminates of 31.5 mm and 100 mm thickness using the prepreg process. However, it is associated with high cost due to the prepreg material itself, the high amount of energy needed for the autoclave pressure-cure cycle, the use of inert gas, and the amount of manual labour still involved. As a process with a one-sided rigid tool and flexible second mould half, the temperature profiles through the thickness are not symmetric along the centre of the laminate [87]. The temperature profiles in the laminate are mainly determined by heat transfer phenomena and are further affected by the bleeder materials and the convective heat transfer coefficient between the vacuum bag and autoclave air [88,89], while they are little influenced by the thickness of the mould assembly [87]. Furthermore, corner thickening/thinning and fibre wrinkling are typical defects on radius sections of prepreg autoclave parts [90,91]. These effects are a consequence of prepreg mass flow and the proportion of fibres oriented along versus across the edge and occur already in the early stages of the lay-up. Increasing laminate thickness and reduced corner radii worsen the effect [90]. As a process with a one-side flexible mould, the autoclave parts exhibit thickness variability caused by material variability of the prepreg itself [91], and inhomogeneous fibre compaction and resin flow due to heat transfer phenomena (see Section 2.2), which are especially critical for thick parts. Therefore, a trend towards out-of-autoclave (OoA) processing is observed to reduce costs [92] as well as the use of new resin systems with smaller reaction enthalpy to reduce temperature overshoot [80,93]. For example, Maguire et al. describes the use of a novel epoxy powder to infuse a 100-ply laminate in a OoA [94]. The resin can maintain a low viscoity of 10–100 mPa s for up to 3 h at 120 °C, which is sufficient to infuse the laminate. Maguire reports a dual scale flow for impregnation in conjunction with a 45% decrease in thickness without a temperature overshoot during cure (see Fig. 4).

Wet winding is commonly used to manufacture pressure vessels with thick-walled segments, which can reach wall thicknesses of up to 74 mm [95]. The strength of the vessels is influenced by (production) parameters such as stacking sequence, fibre tension, production time, resin viscosity and fibre tension gradient [82,96]. Above all, a high fibre volume content in the hoop layers tends to result in a higher vessel strength [82]. Ha et al. investigates delaminations that occur during the curing of wet-winded thick-walled laminates and determines the resulting residual stresses using strain gauges, applied as circumferential segments are cut from the laminate [95].

2.1.3. Process with simultaneous fibre placement and fibre impregnation

Pultrusion is an established process for the efficient production of thick-walled fibre composite profiles. In thick-walled laminates, temperature gradients caused by the exothermic reaction are also problematic here, leading to residual stresses during curing [97]. Furthermore, Yuksel et al. shows that a non-uniform fibre volume content distribution occurs in pultrusion profiles (cross-section 19.5 × 19.5 mm^2), reporting a lower fibre volume content in the core compared to the edge layers [98]. The residual stresses for unidirectional (UD) pultrudates can be simulated by modelling at the meso level, taking into account the local differences in fibre volume content and reaction kinetics. Wet pressing is a liquid impregnation process, but is listed in this category because the fibres are simultaneously shaped and impregnated during the pressing process. Due to the predominant impregnation in the thickness direction, wet pressing is rather unsuitable for thick-walled laminates due to the effect of hydrodynamic compaction of the fibres.

2.2. Process simulation

The main challenges arising in the manufacturing of thick composites are related to fibre compaction, resin flow and curing (see beginning of Section 2.1). Therefore, significant effort has been taken to predict these phenomena in order to establish filling strategies and process cycles to avoid trial and error. Depending on the mould (rigid or flexible) and the fibres (dry or pre-impregnated) effects of fibre compaction, impregnation and curing follow one after another or simultaneously which determines how process simulation must be approached (Fig. 5).

Dry fibres and rigid tooling (without noteworthy flexibility) represent the most straightforward case as the fibre compaction, resin flow (permeability values required), and curing occur in succession. In the other variants (b–d) there are interactions that must be considered in process simulation. Aspects of these simulations specific to thick-walled laminates are detailed below.

2.2.1. Nesting and fibre architecture

The fibre tows and layers of fabrics form a porous structure that is compressed to achieve the desired fibre volume content. The thickness of the compressed fibre stack is always smaller than the sum of the individual uncompressed fabric layers [99], because the fibres are elastically compacted and fibres interact, slightly changing their shape and location, when subjected to transverse compression forces. The latter effect is called ‘nesting’. The compaction behaviour is described in literature by several authors, e.g. for dry fabrics in [58,100,101] and for impregnated fibres in [60,102]. The effect of nesting increases with the number of fibre layers, which tend to be numerous in thick composites. It also varies based on the type of textile used. E.g. Chen et al. [101] provides an analytic formula to calculate the amount thickness reduction due to nesting dependant on the number of fabric layers for woven fabrics.

X-ray computed tomography (XCT) is an effective method of visualising fibre architecture at a mesoscale, even under varying compaction conditions. Thus, XCT enables the in situ analysis of changes in the geometry of the tow, inter-tow gaps and variations in the internal structure of thick composite materials under different compaction conditions [56,57]. With the help of fibre architecture modelling software, e.g. TexGen [58,103], a meso-scale model can be created for structural simulation representing structural effects due to nesting. Results

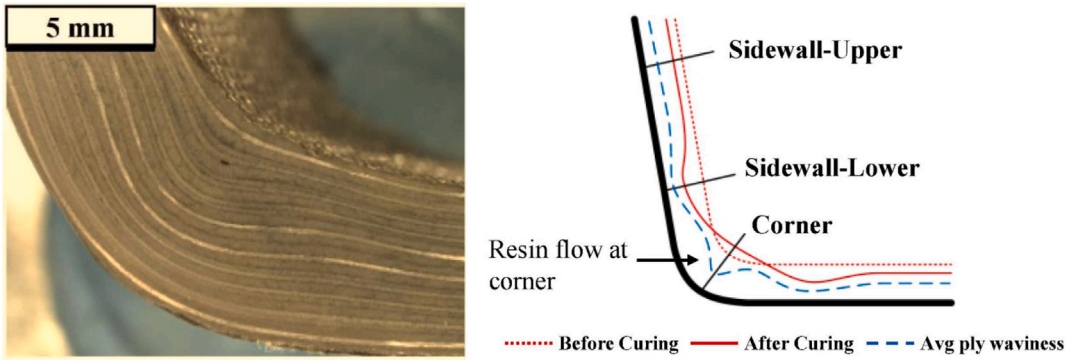

Fig. 4. Autoclave consolidation effect: (left) corner of laminate with 60% of fibres along the edge, 30% in ±45° orientation and 10% of fibres across the edge [90], (right) schematic of corner profile after autoclave curing [90].

tooling	dry fibres	wet fibres
rigid	(a) RTM process: - compaction simulation - permeabilty determination - filling simulation (unsaturated flow), potentially taking into account fiber wash out - curing simulation	(b) prepreg and SMC hot press process: - compaction (for SMC with intended flow of fibers) - in combination with temperature dependant viscosity change of matrix - in combination with onsetting
flexible	(c) VARI, VAP process: - compaction simulation - permeabilty determination - filling simulation (unsaturated flow) - post-filling thickness equlibration in combination with cure	(d) prepreg (out-of) autoclave process: - compaction in combination with temperature dependant viscosity change - in combination with saturated flow - in cominbation with air evacuation - in combination with void formation - in combination with ongoing cure

Fig. 5. Overview of the process phenomena and their interactions that must be taken into account in the simulation, depending on the tool and semi-finished fibre product.

from computation intensive meso-scale models can be implemented in functions for simulation of larger parts on macro-scale. Draping simulation focuses on draping planar textiles into 3D-shape accounting for large shear deformations that are the cause of wrinkles, but usually does not include compaction effects. Thompson et al. includes linear through-thickness compliance into finite element analysis based draping simulation by capturing surface interactions and by adapting pressure over-closure relationships of penalty contacts [100]. Thus, his model is able to predict the location, shape and magnitude of wrinkles in a radius section during vacuum bag compression of 24 layers of carbon plain weave. The formation of out-of-plane and in-plane wrinkles is described (Fig. 6a–c).

2.2.2. Resin flow

Impregnation of dry fibres in liquid-composite moulding takes place as a non-saturated flow [103]. In order to accurately simulate the filling process of thick-walled composites, it is imperative to consider the permeability differences that occur across the laminate thickness [104]. These differences are a consequence of inhomogeneous compaction of fibres and textiles. Therefore, volume elements which can reproduce flow in thickness direction and principal permeability values in-plane and in through-thickness direction are required [105]. The required permeability values can be measured either by means of experiments or purely virtually using the aforementioned X-ray computed tomography coupled with a flow simulation through porous media [56]. Saouab et al. [56] and Ali et al. [57] highlights that thicker reinforcements undergo significant deformation under compaction, affecting their permeability. Saouab et al. [56] found that the virtual permeability computation using voxel models offers high accuracy compared to methods like stochastic virtual modelling or simplified geometry approaches. However, voxel-based methods are computationally demanding, and extracting representative unit cells is challenging due to the need to address periodicity. In contrast, stochastic models can approximate the heterogeneous structure of thick laminates with significantly lower computational cost and without the need for image segmentation, although they do require specialised geometric modelling and meshing tools. For the purpose of filling simulation, commercial software such as PAM-RTM or RTM-Works [106,107] can be used by assigning appropriate permeability values to regions with varying levels of compaction. Fibre washout, referring to the dislocation of the fabric caused by high infiltration pressures commonly encountered in the HP-RTM process, remains beyond the predictive capabilities of these models. Therefore, the authors of [108] developed a one-dimensional model based on a statistically permissible stress field within the preform material and the application of beam buckling theory to predict fibre washout as a function of process variables such as clamping force and injection pressure. The model indicates that fibre washout is most pronounced at the onset of the injection process. However, a comprehensive prediction of fibre washout at the macroscale

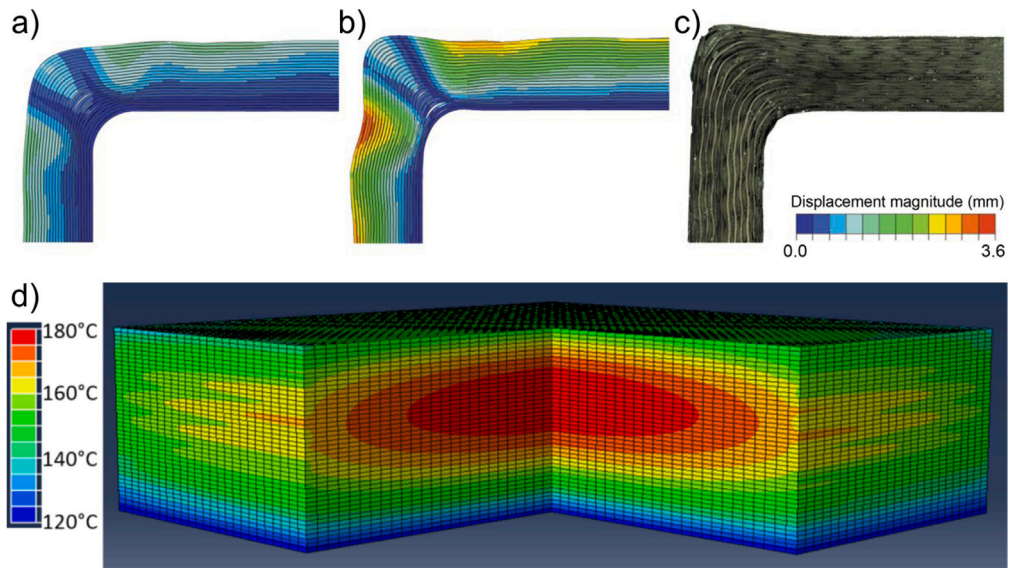

Fig. 6. Selected examples of process simulation for thick-walled laminates: draping simulation of radius section (a) with perfect contact between plies [100], (b) with extra bulk [100], (c) experiment [100], (d) Thermal analysis temperature plot of a 30 mm carbon/epoxy laminate during a temperature overshoot event in an oven cure process at 120 °C [80].

remains an open challenge, necessitating future investigations into meso-scale tow movement.

2.2.3. Thickness variability

With the use of tooling with a flexible membrane, like in VARI, VAP or the prepreg process (conventional autoclave and OoA), laminate thickness changes during the process while the fibres are already impregnated with resin. Thus fibre bed compaction in combination with temperature and cure dependant viscosity changes of the matrix needs to be considered. Therefore a thermo-kinetic modelling approach is necessary. The authors of [52,109] describe the post-filling thickness equilibration after dry fibre impregnation in the VARI process. Trochu et al. presents a numerical model for fibre bed deformation enabling the prediction of thickness variations during the VARI process at the macroscale [59]. The approach employs three-dimensional adaptive mesh refinement in conjunction with an extrusion algorithm to generate a locally refined 3D mesh with a reduced number of elements, thereby enhancing computational efficiency. This methodology facilitates the incorporation of geometrical features such as flow channels to account for edge effects (e.g., race tracking). The final 3D mesh with multiple stacked layers is created by mesh extrusion, allowing for easy setting of through thickness parameters for each layer. Bodaghi et al. provides a comprehensive review of the above described variability of permeability, particularly focusing on how reinforcement distortions and dual-scale flow mechanisms influence mould filling and final part quality in liquid composite moulding (LCM) processes [104]. It further details state-of-the-art simulation techniques, including finite element models, stochastic simulations, and flow behaviour modelling, that account for variations in fibre architecture, nesting, tow waviness, and permeability fluctuations. In thin laminates the thickness equilibration time is usually significantly shorter than the gel time of the resin. However, for thick laminates due to low thermal conductivity in thick sections, heat build up could lead to pre-mature gelation before thickness equilibration is reached. For liquid composite moulding processes, the gelling ratio, defined as filling time /reaction time, can be used to assess whether this is critical [25]. With prepreg material, the matrix is already in a partially cured (B-stage) state and undergoes further curing and associated viscosity changes at temperatures above −18 °C. During the cure temperature cycle the viscosity of the resin needs to become sufficiently low, especially in out-of-autoclave processes [110]. Thus the out-time and exposure to room temperature before final cure are critical, especially as the lay-up of large, thick components made from prepreg material can extend over several weeks [111], the increase in viscosity at room temperature must be taken into account. The tracking of changes of B-stage glass transition temperature and total heat of reaction by differential scanning calorimetry (DSC) and measurement of minimum viscosity by rheometry are means to monitor the state of the prepreg [110]. The cure of thick section composites made from prepreg has been extensively studied in [60,61,63].

For prepreg processing, Li et al. applies the Gutowski fibre bed compaction model within a finite element framework to simulate coupled resin flow and laminate compaction during curing process [60]. The results demonstrate that resin velocity variations influence laminate thickness and deformation, with predictions aligning well with experimental data. Furthermore, the authors shows that compaction respectively fibre volume content differences across the thickness of a 4 mm prepreg laminate occur with values as high as 70% at the outside and as low as 55% in the middle, highlighting the necessity for optimised cure cycles to achieve uniform compaction and high-quality thick laminates.

2.2.4. Curing

Modelling of curing is the most widely researched sub process of the composite manufacturing sequence with several publications for thick composites starting as early as in the year 1991 [36] up to now [45,112].

The modelling approaches can be divided into 0-dimensional (solving a system of differential equations without thickness resolution) [31], one-dimensional models (temperature profile across thickness at one location in the laminate) using 1D finite differences [94,113], 1D finite element models (FEM) [45,114], two-dimensional (temperatures in one cross-section of the laminate) using finite differences [29,36], finite elements [64,88,115], with commercial FEM software PAM Cure [32] or multiphysics software Comsol [25], and using 3D FEM [80,112], with commercial software Ansys [114]. Cure simulation for laminates up to 40 mm thickness was carried out in [31]. Esposito et al. experimentally measured the highest temperatures at the surface and the centre of prepreg laminates of different thicknesses during curing and predicted the temperature over time with his model to link overheating with interlaminar shear strength degradation [32]. For a 25 mm thick laminate the measured difference of surface and centre temperature was 44 K, with local temperature variations in the centre of 87 K. Esposito's

model was in very good agreement with the experimental data of temperature and interlaminar shear strength tests. This clearly highlights the enormous temperature gradients present in thick laminates and the influence on mechanical properties of the final laminate. Overheating reduces interlaminar shear strength in thick FRP laminates [32]. Spatial cure gradients depend on part geometry and direction-dependent heat transfer [36], therefore, temperature gradients should be simulated at critical cross sections. The reviewed literature shows, optimised cure cycles reduce temperature and degree-of-cure gradients by up to 39% [112] and as a result residual stresses [25,31].

In conclusion, thermal management for curing thick composites is crucial due to low thermal conductivity of the reinforcement and exothermic resin curing. Thick composites require special processing techniques to ensure uniform quality, to control heat build-up and avoid defects and matrix degradation [63,64]. Cure cycles must be carefully designed to balance laminate temperature and fibre compaction. Accounting for anisotropy arising from different fibre orientation in the laminate architecture enhances the accuracy of temperature and curing kinetics predictions in curing simulations [61,64]. To reduce thermal gradients, the cure cycle must use slow heating rates and lower dwell temperatures, resulting in longer process cycles [49]. Fibre compaction affects heat dissipation, because a higher fibre volume fraction improves thermal conductivity. If laminate compaction is incomplete, excess resin remains trapped, leading to higher exothermic heat build-up at the centre (temperature overshoot, (Fig. 6d)). The review shows that different modelling approaches (1D, 2D, 3D) trade computational efficiency for accuracy. Multiphysics modelling and optimisation techniques (genetic algorithms, multi-physics models) improve prediction capabilities and thus the cure cycle efficiency.

2.3. Process monitoring and quality inspection in the production of thick-walled FRP

In-situ process monitoring based on non-destructive testing methods is increasingly being used to continuously monitor production and guarantee the production quality of FRP components [116]. However, this is still largely at the research stage for the production of thick-walled FRP and rapid manufacturing processes. One focus of the research here is on the detection of the matrix flow front during the infiltration process in the HP-RTM process and the detection of misorientations of the fibres [117,118]. Some work has already been carried out in recent years on resin flow front detection. For example, in [119,120] the flow front was detected at various points in the HP-RTM mould using capacitive measurement technology. It is also possible to locate the flow front using contact ultrasound in transmission (through the entire thickness of the RTM mould) by measuring the signal amplitude and sound velocity [121,122] . However, this method cannot be used if only one-sided access to the mould or complex-shaped moulds are used. One way of detecting the flow front within a complex mould is to examine the multiple reflections of a longitudinal wave using a line-array sensor. This involves combining a large number of piezo elements in a phased array probe, which can be used to direct and focus the sound field by delaying the transmission of the individual elements [123]. The ultrasound can be focused on any area of the fibre material by controlling the transmitting elements arranged along a line in the probe accordingly. Due to the larger dimensions of a line probe compared to that of a single transducer, multiple reflections can be detected simultaneously at different points on the mould. Depending on the degree of infiltration, a progressive flow front can be detected. The pulse-echo method not only makes it possible to determine the filling level in the plane, but also in the thickness direction. With the help of single transducers, such a filling level determination has already been realised in several works (see, for example, [124]). When manufacturing thick-walled FRP, it should be noted that the risk of defects occurring in the laminate increases with increasing laminate volume [125]. This is discussed in [126] at the materials level using test specimens of different dimensions and in [127,128] at the component level on FRP rotor blades of wind turbines. These production-related defects include pores, inclusions, surface defects, fibre misorientation, and resin-rich as well as resin-free areas [125]. In addition to the known fibre misorientation in the laminate plane, known as fibre waviness (Fig. 7), fibre undulations out of the laminate plane, known as undulation, occurs with increasing number of layers in thick-walled FRP.

Micrograph analyses, X-ray methods and the embedding of optical fibres can be used to detect and analyse such fibre defects [131]. The causes for the formation of undulations are manifold and can be found in [40] among others. The author does not explicitly address thick-walled laminates. In thick-walled multilayer composites manufactured using the braiding process fibre misalignments occur because the inner layers form an uneven base for the subsequent layers [132]. A process-related inhomogeneous fibre distribution also occurs when several layers of different orientation are laid down (nesting) [133]. Fibre misalignments also occur when the preform is inserted into geometrically complex tools. This creates local manufacturing defects such as overlaps, fibre gaps and undulations, which result in varying fibre orientations and fibre volume contents of the FRP [134]. Furthermore, the individual layers are compressed differently, resulting in different frictional behaviour between the layers [130]. In addition to the composite imperfections caused by textile processing, fibre displacements are also caused by infiltration processes [135]. The HP-RTM process, in particular, can cause fibre displacement due to the high resin flow rates during impregnation [136], resin-rich regions and voids in thin-walled laminates [137].

The flow of the low-viscosity resin through the fibre structure in the cavity can be compared to the flow of a Newtonian fluid through a porous medium in terms of fluid mechanics [138–140]. Mathematically, the flow process can be described using Darcy's law. It describes the flow velocity as a function of the viscosity of the resin mixture, the permeability of the semi-finished product and the pressure gradient between the inlet and outlet. Permeability describes the transmission resistance of the fibre structure to the fluid flowing through it. It depends on the type and architecture of the textiles and their compression in the cavity [141]. For a realistic description of the impregnation behaviour in thick-walled FRP, the permeability in the thickness direction is of central importance [142,143]. Another cause of fibre misalignment is shrinkage, which is caused by the chemical cross-linking reaction and cooling of the thermosetting matrix. Studies show that this leads to compression and deformation of the fibres [144] and induces residual stresses [35,145]. This effect is more pronounced in thick-walled laminates, as the heat of reaction is dissipated relatively poorly. This results in an uneven temperature distribution and inhomogeneous curing [146]. With greater wall thicknesses and the associated larger matrix quantities, the process-related infiltration and curing parameters (temperature, pressure) have a significant influence on the resulting material properties. Three-dimensional stress states with non-negligible compressive stresses transverse to the laminate plane occur with increasing frequency [147,148]. The state of research on the definition of suitable curing cycles in the production of thick-walled FRP laminates is described in [149,150]. In summary the degree of cross-linking, respectively the glass transition temperature, and the fibre volume fraction are identified as key performance indicators for achieving optimal curing [151]. In addition, in contrast to thin-walled laminates, a homogeneous temperature distribution within the laminate is only possible to a limited extent with larger matrix quantities due to the exothermic curing reaction. In the works [41,152] these inhomogeneous temperature curves are described for prepreg systems and were evaluated on the basis of experimental investigations of the mechanical in-plane tensile and compressive strengths. The design of thick-walled laminates can therefore not be carried out according to the classical laminate theory, as the "interference stresses" in the form of normal stresses and interlaminar shear stresses in the thickness direction make a more complex stress and strength analysis necessary [153].

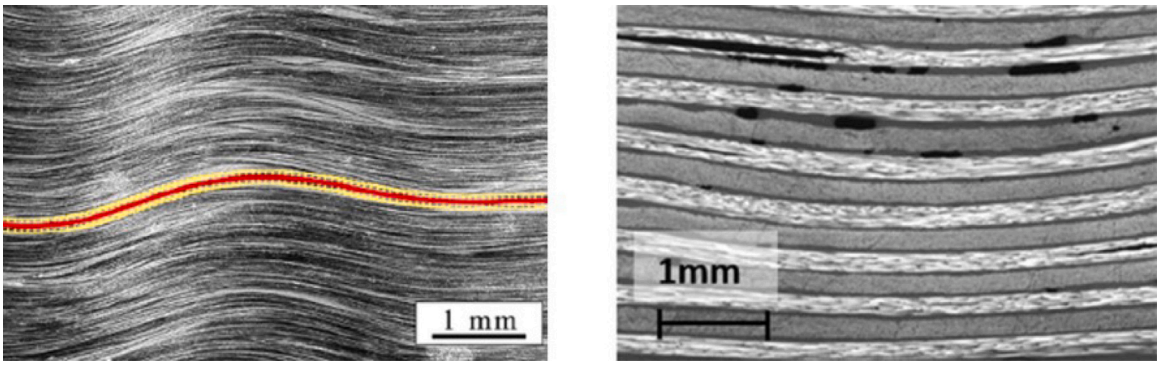

Fig. 7. Unidirectional carbon fibre reinforced epoxy resin with fibre waviness (in the laminate plane, left) [129] and undulations (in thickness direction, right) [130].

3. Mechanical testing of thick-walled FRP

The evaluation of the influence of thickness and manufacturing-related imperfections is often carried out using mechanical tests under quasi-static, dynamic, and cyclic loading and is summarised in the literature under the term "size effect" [24]. It is assumed that the specimen or component size has an influence on the mechanical properties of the material used, especially its strength, and it is questioned whether the transfer of characteristic values from standardised (thin-walled) test specimens to other size scales is possible without further ado [154,155]. Although detailed work on the topic of the size effect and its description of a wide variety of brittle materials can be found in the post-World War II period, the growing interest in fibre composite materials for load-bearing elements has also led to an increase in research work on this topic since the early 1990s. Based on the failure behaviour of brittle materials, two theories have been (further) developed to explain such an effect:

- Statistical size effect: The basis of this theory is the weakest-link principle, which is based on a random, statistical distribution of material strengths in a body (mainly using a Weibull model [155]).
- Fracture mechanical size effect: The scale law, which was largely characterised by Bažant, is based on an imbalance between the released strain energy stored in the body at the crack front and the fracture energy required for crack propagation [156].

It should not go unmentioned at this point that a variety of factors (or even a combination of them) can, of course, have an unfavourable influence on the failure of thick-walled laminates. Last but not least, the following should be mentioned in this context:

- The influence of manufacturing (see Section 1),
- Test conditions such as clamping and load introduction,
- Free edge effect (in the case of varying layer orientation),
- Stress gradients under bending stress and
- Self-heating effects with cyclical load.

3.1. Quasi-static behaviour

Most of the experimental work in this field deals with behaviour under quasi-static loading. The tensile and flexural strengths [157–163] and the compressive strengths [164–167] decrease with increasing sample volume. The cause of this is attributed to fibre waviness and deviating alignment of fibre to load direction, which primarily occur in the laminate thickness direction. A good summary of the work in the decade between 1990 and 2000 can be found in [168], a widely cited article on this topic. Based on this and several other comprehensive literature summaries (e.g. [169,170]), the individual papers from this period will not be discussed further. However, it should be summarised that the size effect occurs independently of the direction of loading (tension, compression, and bending). The failure mode and its existence are essentially explained and described by statistical phenomena and models, largely Weibull distributions, which describe the material behaviour sufficiently accurately in the majority of works [171]. In particular, for compression tests [164,172], significant variations in strength are expected, due to the well-known complex boundary conditions in compression tests [22].

Table 1
Overview of the testing standards and the maximum wall thicknesses specified therein.

Load type	Standard	Wall thickness in mm
Tension	ISO 527-4 [179]	2–10
	ISO 527-5 [180]	1–2 (UD)
Compression	ISO 14126 [181]	2–10
Bending (3-/4-point)	ISO 14125 [182]	2–4
Shear (45° tensile test)	ISO 14129 [183]	2

In this context, useful specimen geometries with corresponding clamping and load application areas are discussed in various publications for thick-walled laminates mentioned below. In principle, specimens up to 10 mm thick are defined for tensile and compression tests in accordance with DIN EN ISO 527-4 and 14126. An overview of existing standards is given in Table 1. However, it is clear that these alone will not lead to good results for thick-walled laminates [173]. In compression tests, even for thin-walled laminates [174,175] large differences can be expected due to the test equipment and specimen geometry. Good examples of this can be found in [176]. Similar solutions are discussed in [177], where the well-known ICSTM load unit for compression specimens (see [178]) is used to address specimen clamping issues.

Among the much-cited works in the experimental field from the current millennium are the studies in [22,173,184]. Here, too, it is shown that thick-walled laminates exhibit comparatively high reductions in strength under compressive loading and that these also depend strongly on the ply structure used. The causes cited for this include fibre waviness and larger production-related defects. However, the degree of fibre misalignment and its influence on mechanical properties are currently difficult to predict quantitatively [144]. The static tensile and compressive loads are also discussed in [185]. A thickness effect can also be shown for certain ply structures under tensile loading, but the maximum investigated laminate thickness is 4 mm and does not indicate the extent of the statistical validation [186]. It is already evident from the specimens analysed in [186] that even with optimised specimens, many failure locations can be found close to the load introduction elements, i.e., the clamping area. However, more recent investigations on samples up to 20 mm thick show no significant drop

in strength under tensile and compressive loading with comparable fibre volume contents in UD-specimens [187]. When investigating the size dependence of the mechanical properties of FRP, it is therefore often unclear whether this is a true size effect of the material [186,188], respectively, the structure [189], or whether other factors are at play, such as a reduction in the quality of production with increasing laminate thickness [168]. A large number of studies can also be found on the quasi-static behaviour of thick-walled laminates under bending load (e.g. in [188,190,191]). The results clearly show how differently UD, cross-laminate, quasi-isotropic and ±45° bending specimens behave with regard to the influence of laminate thickness. No clear influence is visible in the UD laminates, while the flexural strengths of the three other multilayer composites are clearly degraded. In contrast, in [188] the reason for this is seen as a probabilistic effect in the bending test series examined. Recent studies have investigated the size effect in the case of interlaminar failure. To this end, they compare the behaviour of specimens of different thicknesses under Mode I and Mode II loading [191]. Again, there is a considerable drop in fracture energy, which can be modelled with sufficient accuracy using linear elastic fracture mechanics.

3.2. Fatigue behaviour

Compared to the behaviour under quasi-static loading, the available data on the fatigue behaviour of thick-walled FRP is not as extensive, particularly with regard to a direct comparison of thin- and thick-walled structures. The following section summarises the findings of the investigations on thick-walled laminates and the comparative investigation of laminates of varying thicknesses.

3.2.1. Fatigue tests on thick-walled laminates

In general, a wide range of literature is available on fatigue investigations of thick-walled laminates. For example, in [192], the author summarises the status quo and describes the difficulties and influencing factors that arise when testing these laminates [193]. It is known that the failure phenomenology differs considerably in some cases from that in thin-walled FRP laminates, as considerable normal and shear loads orthogonal to the laminate plane are to be expected in thick-walled laminates, which is why delamination is often dominant. The poor heat transfer due to the generally poor thermal conductivity of fibre-reinforced composites also contributes to a different failure pattern [194]. A considerable increase in temperature in thick-walled laminates is expected even at low load frequencies, especially under tensile and compressive loads [195]. It has also been shown that neither established fatigue life models nor progressive damage models or empirical models can adequately predict the damage development and service life of thin-walled FRP. In [196] a hybrid model with good agreement between experimental and theoretical data under bending load is presented on this topic. Further investigations are described in [197] in which the author comprehensively describes the fatigue behaviour of UD-specimens made of glass fibre reinforced polymer (GRP) under bending swell loading. Although the influence of laminate thickness is not directly described, the specimens are thicker, with a laminate thickness of approx. 6 mm, and various very useful statements on improving the specimen shape with regard to 3D effects (e.g. anticlastic bending) can be found. In addition, the work contains many further suggestions for improving the understanding of thick-walled bending specimens. Fatigue tests under bending load can also be found in [198] on woven GRP laminates with a wall thickness of 15 mm. This shows that the deformation and the loss of stiffness increase steadily over a long period of time and only increase very sharply just before failure. The stiffness normalised to the initial stiffness decreases almost linearly with the number of load cycles. Furthermore, the fatigue behaviour of thick-walled laminates made of carbon fibre reinforced polymer (CFRP) with tough intermediate layers under load in the thickness direction is also being investigated [199]. However, there is no comparison with data from thin-walled laminates to assess the potential influence of wall thickness on fatigue behaviour. Fibre architecture in general has a significant influence on the fatigue properties of FRP [200], but fibre misalignments, in particular, reduce the service life [201].

3.2.2. Comparative tests on laminates with varying thicknesses

One of the first comparative studies can be found very early on. As early as 1979, the first probabilistic considerations on the scaling effects of open-hole CFRP specimens under cyclic compressive loading were made in [202], but without presenting experimental results on thick-walled laminates. In 1988, the first experimental investigations in [203] established that under cyclic bending load with a stress ratio (R) of 0.1 and a frequency (f) of 1.2 ...3 Hz there is a decrease in the bending strength of laminates of different thicknesses (up to 20 mm). A summary of the experimental results is shown in Fig. 8, left. This shows a shift of the Wöhler lines to the bottom left, where the authors achieve a reasonably good prediction of the thickness influence with a simple Weibull model. Unexpected results are described in [204] when investigating the damage behaviour under alternating load ($R = -1$) before and after low-energy impact of compression specimens with scaled stacking $([0/45/90/-45]_{ns}$ with n = 2,4,6; where $t_{n=1} = 1$ mm). Interestingly, not only the pre-damaged, thick-walled specimens, but also the undamaged specimens show a more resilient behaviour in the fatigue tests (cf. Fig. 8 middle). No explanation is given for this unexpected result. The result is particularly surprising considering the comparatively high test frequency, which was f = 10 Hz for all tests in unison. A considerable self-heating effect is probably already present here [205]. Furthermore, [206] examines the fatigue behaviour of 32 mm thick laminates. Major efforts are mentioned here in order to avoid the clamping problem. The results for specimens under pure tension-swell loading give the impression that a thickness effect is present at higher loads, but this is apparently not found at lower load levels. In a recently published study, the influence of the size effect at different load ratios on UD-laminates of different lengths under 0°, 10° and 90° loading direction (f = 5 Hz) is analysed [207]. The specimens appear to correlate well with a Weibull distribution related to the volume.

However, none of the works cited above consider the influence of self-heating as an influencing factor. Various publications point out that there are indications of strong heating of the inner layers under fatigue loading even at the lowest loading frequencies [205,208,209]. A series of data on the size effect with additional consideration of self-heating can be found above all in [195,210–212] on UD-specimens under pulsating tensile and compressive loading. In an attempt to account for the influence of self-heating by using a lower test frequency (10, 5 and 2 Hz, respectively) and thus gain a better understanding of the pure size effect, the failure behaviour was tested at three different wall thicknesses (4, 10 and 20 mm). The shift of the S-N curve to a lower stress level was found to be significantly smaller for the first increase in wall thickness compared to the second, Fig. 8 right.

The reason for this is believed to be the reduced manufacturing quality of the 20 mm thick laminates. Furthermore, [208] proposes an FE model to predict self-heating. The use of this model gives reasonably good results compared to the temperature increases recorded in the experiment [195], which are, however, very high (well above $\Delta T = 10$ °C). Although the conclusions regarding the size effect are consistent in this sense, an influence on the failure behaviour in general can nevertheless be assumed here. In this context, it is worth mentioning that there are specific studies on the self-heating of fibre composites, including comparative studies on the varying sample thicknesses (e.g. [205]). However, since all of these studies consider the self-heating effect in isolation and the fatigue behaviour is, in some cases, standardised to the maximum number of load cycles endured, it is not possible to draw any conclusions about the size effect. In conclusion, it can be stated that thick-walled FRP also tend to fail prematurely under cyclic loading.

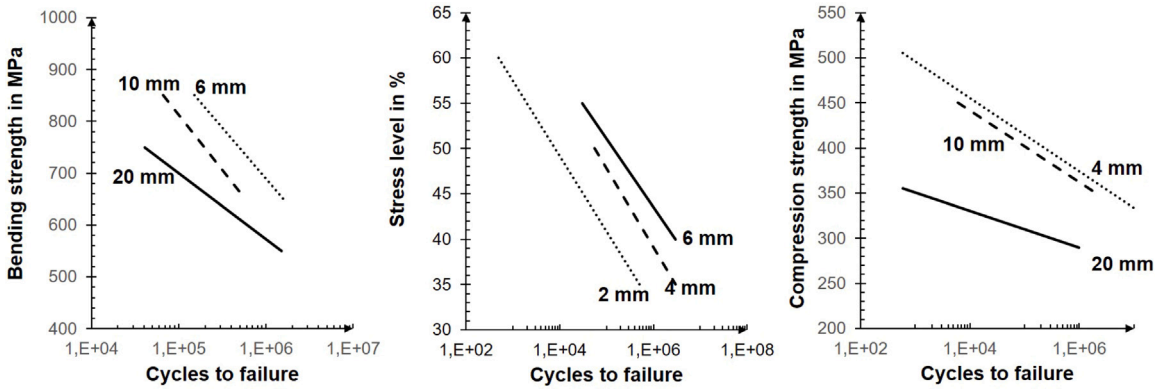

Fig. 8. Exemplary course of the Wöhler curves with varying specimen thickness according to [203] (left), [204] (middle) and [195] (right).

However, simply extracting the size effect is problematic due to the wide range of influencing factors. The main one is self-heating, which is added to the boundary conditions known from quasi-static testing. The results of the existing literature show that it is hardly possible to consider only one of these effects exclusively. Switching to such low load frequencies that the self-heating effect has no influence is impractical and generally does not do justice to the specific application. Thus, the fatigue behaviour of thick-walled fibre-reinforced polymer composites can only be described safely and reliably as a combination of these two factors. Some attempts have been made in this respect, although a holistic description of both effects is currently only available to a limited extent.

3.3. Impact behaviour

Impact tests are classically divided into low-velocity, high-velocity, and hyper-velocity impacts. According to [213], the corresponding impact velocities are v < 10 m/s, v < 1000 m/s and v > 1000 m/s.

3.3.1. Low-velocity impact

There are a large number of studies that perform low-velocity impacts (LVI) on FRP specimens of different thicknesses [214–222]. When investigating the influence of laminate thickness on impact behaviour, mainly two different approaches are used. Some publications [217,218,222,223] use a constant impact energy that is independent of the thickness of the specimen. Alternatively, an impact energy per thickness of the test specimen is specified [214,224–226]. As intuitively expected, LVIs with a constant impact energy cause less damage, delamination, fibre breaks, etc. in thick-walled laminates than in thin-walled specimens. Furthermore, a higher number of repeated impacts is required to cause the same damage. The studies do not establish a more precise correlation between specimen thickness and damage size at constant impact energy [217,218,222,223]. For better comparability between component thickness, impact energy and damage pattern, impact energies per layer or per millimetre are used in many studies. After analysing around 500 LVI tests, the authors in [227] found that the relationship between the critical damage initiation force P_{cr} and the component thickness t correlates in the form of $t^{3/2}$; this relationship was confirmed by several studies [224,225,228,229]. The higher damage tolerance with increasing specimen thickness can be described by a change in the damage behaviour. In the case of thin-walled specimens, which are generally less rigid, the impact causes a globally occurring bending. This bending causes tensile stresses on the bottom side and compressive stresses on the top side. Consequently, the lower layers usually exhibit tensile fractures, while a compression or shear failure develops on the upper side. In this case, the damage grows from the bottom to the top of the specimen.

With thick-walled specimens, the impact load results in a greater contact force due to the higher stiffness. However, only a local bending moment occurs in the upper layers, not a global one. The resulting stresses cause matrix fractures, also known as shear fractures, to form in the upper layers, which are arranged at an angle to the central layer, and delamination. The damage then grows from top to bottom throughout the specimen [225]. The damage growth for thick-walled specimens is therefore the opposite of that for thin specimens. A comparison of the different damage growth can be found in Fig. 9. In subsequent compression-after-impact (CAI) tests, the bottom layer of thin specimens buckles quickly due to delamination, leading to a drastic reduction in residual strength [220,230,231]. In thicker specimens, delamination occurs uniformly throughout the width of the material, but is usually stopped at the interfaces of two different layer orientations [220,221,225]. Therefore, larger sub-laminates are present in a CAI test, which can absorb the resulting forces, resulting in increased residual strength [220,230–232]. In addition to the difference in damage behaviour, inhomogeneities in the material have a significantly greater negative effect on the impact behaviour of thin specimens than thick specimens [219]. Furthermore, the thickness of the specimen has a greater influence on the impact behaviour than other dimensions of the specimen [233].

3.3.2. High-velocity impact

The relationship between specimen thickness and impact behaviour with high or hyper velocity impacts has been little researched to date [234]. Most studies in this area [235–240] agree that, for the same impact energy, an increase in the thickness of the specimen leads to higher maximum energy absorption per layer. Only in [241] this behaviour is observed for parts of the measurement series. The improvement in impact behaviour can be explained by a change in damage behaviour. For specimens thicker than 10 mm, the damage behaviour can be divided into several steps (see Fig. 10). First, the impact of the projectile causes the specimen to form delaminations throughout its thickness. The projectile then penetrates the specimen without any major deflection until a sublaminate forms on one of the delamination surfaces. The sublaminate is then subjected to a bending load and fails completely or partially due to tension. However, in thin-walled specimens, delaminations occur after impact of the projectile. Due to their low thickness, they cannot form sublaminates and subsequently fail due to bending [235]. For hybrid set-ups [242] investigated the thickness effect and impact damage behaviour of carbon/Kevlar fibre-reinforced laminates, revealing a critical threshold thickness beyond which the dominant failure mechanism changes. For thinner plates, placing Kevlar layers at the back improves impact resistance, but once plate thickness exceeds a certain limit, this configuration becomes less effective. Furthermore,increasing the Kevlar fraction reduces the threshold thickness, as shear plugging in carbon layers decreases and larger deformation occurs in aramid layers. These findings offer important guidelines for designing and optimising hybrid laminates in various applications, such as aero-engine fan casing and armour protection.

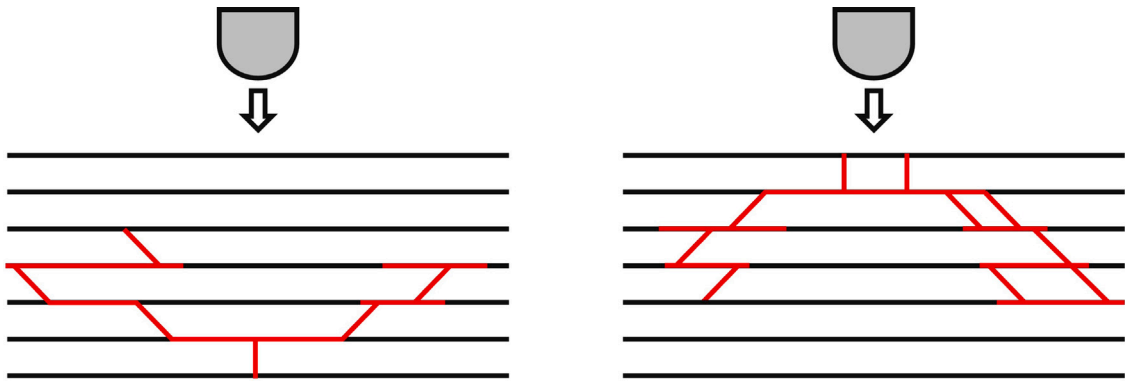

Fig. 9. Schematic representation of different impact damages (shown in red) after a low-velocity impact in thin-walled (left) and thick-walled (right) specimens according to [216].

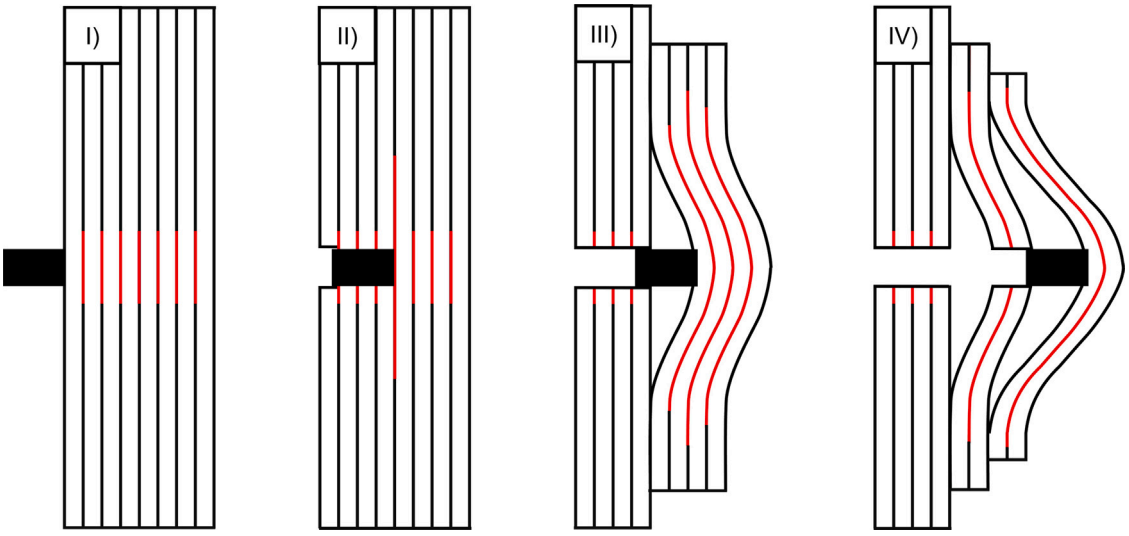

Fig. 10. Damage mechanisms of thick-walled specimens during a high-velocity impact according to [235]: (I) Delamination, (II) Projectile penetration, (III) Formation of sublaminates, (IV) Failure under bending load.

4. Numerical modelling of thick-walled FRP

The numerical investigation of size and thickness effects in FRPs has gained considerable attention because of its potential to optimise mechanical properties and structural performance. Key research areas include finite element modelling, parametric studies of thickness effects, and size-dependent fracture mechanics. In particular [243,244] highlight that the size effect as a crucial factor in modelling the compressive failure of laminated composites, and its proper consideration in simulations is essential for accurate structural predictions. It is shown that micromechanical theories like Weibull-type scaling approach are useful to describe the size effect. Furthermore, multiscale finite element models are useful to study the impact of structure size and stress gradients. Additionally, a longitudinal weak-link model suggests that larger samples are more likely to contain fibre misalignments that lead to early failure.

Advanced numerical approaches, such as three-dimensional mesoscale simulations and cohesive zone modelling, have proven effective in capturing complex damage mechanisms under various loading conditions. For example in [245] a hierarchic 3D finite element for calculating the full stress tensor in composite structures is presented. The element is based on the 3D linear elasticity theory and uses the material law and the 3D equilibrium equations and can be used to efficiently analyse thick-walled composite structures. In [246] it is shown that cohesive zone modelling can reveal how size effects depend strongly on initial crack geometry and orientation in short fibre–reinforced composites, extending these insights to representative volume elements (RVEs) where fibre–matrix debonding further amplifies the overall scaling behaviour. Likewise, experiments with single-edge-notched carbon-epoxy twill laminates [247] demonstrate a clear reduction in nominal strength with increasing specimen size, accurately described by Bažant's size effect law. The authors highlight the importance of measuring the intra-laminar fracture energy (G_f), thus underscoring the role of a realistic fracture process zone for reliable crashworthiness simulations.

In addition, other researchers have explored how variations in fibre thickness and length influence damage evolution and overall fracture performance. For instance, [248] have incorporated statistical size effects into finite element models by treating material properties as probabilistic variables. Typically, Weibull distributions represent the local variability in the strength of the material, reflecting the increased risk of critical flaws in larger or thicker specimens. An alternative strategy uses Monte Carlo simulations combined with micromechanical models, such as a 3D shear-lag framework that accounts for matrix yielding [249]. By integrating measured fibre strength distributions across multiple gauge lengths, these methods capture localised clusters of fibre breakage and outperform traditional Weibull models. The so-called Weibull-of-Weibull approach, in particular, has successfully predicted size-dependent strength in unidirectional CFRPs, aligning with experiments and reinforcing the consensus that composite strength diminishes as specimen dimensions grow.

In addition, researchers have begun to address manufacturing-induced thickness-dependent defects in their numerical studies. For example, [250] employed compaction simulations and micromechanical analyses to examine the influence of nesting in plain-woven CFRP-laminates with varying thicknesses. By generating multiple representative unit cells (RUCs) and applying periodic boundary conditions, they demonstrated that accounting for nesting is crucial to accurately predict damage evolution and stiffness degradation. Relying solely on single-ply or simplified multi-ply configurations can overlook key nesting effects, thus highlighting the importance of including these manufacturing details in any comprehensive computational model.

Furthermore, recent studies have also demonstrated that nesting effects significantly impact the mechanical behaviour of textile-reinforced composites. The interlaminar shear strength and overall failure behaviour of these materials are closely linked to the degree of nesting, as increased nesting can lead to enhanced load transfer through interlocking of adjacent layers, but may also introduce stress concentrations. Experimental results indicate that out-of-plane compression can alter failure initiation mechanisms differently, emphasising the need for detailed multi-scale characterisation to capture these complex interactions [251].

To gain deeper insight into these effects, researchers have utilised advanced experimental and numerical techniques. Experimental techniques to identify the nesting behaviour of textile reinforcements using advanced in-situ CT analysis. Multi-scale modelling approaches, incorporating bi-layer RUCs generated with TexGen, have proven effective in simulating the heterogeneous damage behaviour of different textile architectures. These methodologies have facilitated improved fracture resistance predictions and enhanced our understanding of the interaction between fabric undulation, nesting, and mechanical performance [252].

Lastly, characterisations of fatigue crack growth behaviour in textile-reinforced composites have further reinforced these findings. Specifically, mixed-mode loading with constant compressive force has been shown to alter crack propagation patterns. By employing finite element analysis and digital image correlation techniques, researchers have successfully quantified the energy release rates indicating a major influence of the textile geometry on the crack propagation. These insights underscore the necessity of considering nesting effects when evaluating the fatigue resistance and long-term performance of composite structures [253].

These findings collectively indicate that purely strength-based or linear elastic fracture mechanics approaches insufficiently capture the quasi-brittle nature of textile composites, emphasising the need for size-sensitive modelling strategies.

5. Non-destructive testing of thick-walled FRP

While in many areas the destructive testing of a specimen is sufficient to assess the reliability of similar components, full non-destructive testing (NDT) of all safety-relevant components is prescribed, particularly in the transport sector (rail, aeronautic, naval). In order to ensure a reliable inspection result, there are various NDT methods that must be selected according to the defect and the materials to be tested. The procedures to be used for a specific case are largely standardised. Various authors have already compiled a further overview of existing research approaches in review articles on NDT [254,255] and structural health monitoring [256]. The basic mechanism in non-destructive testing lies in the interaction of an incident wave with the intrinsic structures of the material. The wave can be both, acoustic and electromagnetic, and the material structure is defined, for example, by interfaces, microstructures or material damage. Due to interaction effects such as reflection, transmission, scattering, refraction or absorption, the incident wave undergoes a change in amplitude or phase. This change is quantified on the basis of the signal of the emerging wave and evaluated with the aid of suitable signal and image processing. This allows the material properties to be derived, the material structure to be described and possible defects to be detected.

The non-destructive testing of thin-walled FRP has been the focus of numerous research questions in recent decades in order to ensure imaging, for example in ultrasonic testing, even for a high degree of anisotropy [257]. The increased attenuation caused by the heterogeneous structure of the FRP makes the testing of very thick-walled laminates more difficult, especially with a high degree of anisotropy. While a FRP laminate is considered thick-walled from a structural-mechanical point of view from a wall thickness of 10 mm, such a limit is much more difficult to set from an NDT point of view. The first publications on NDT on thick-walled FRP appeared at the end of the 1980s. In [258], reference is made to the investigation of glass fibre reinforced polymers with a thickness of 50 mm. A clear limit is not specified. A pragmatic approach is proposed in [259]. Here, a test specimen is considered thick-walled as soon as the signal-to-noise ratio (SNR) of a given NDT method falls below an arbitrarily chosen value. The problem with this approach is that a test specimen can be categorised as either thick-walled or thin-walled, depending on the test method and the corresponding attenuation of the material. As this can be very misleading from a structural mechanics perspective, the aim of this review is to provide an overview of the wall thicknesses that can be analysed using the most common NDT methods. This also reflects the definition problem mentioned above, as the studies presented here deal with test specimens between 3 mm and 150 mm, depending on the test method and the defect to be detected.

In general, NDT methods are categorised into surface and volume methods, which already allows a rough estimate of the testability of thick-walled components [260]. For thick-walled FRP, volume methods, including ultrasonic testing and radiographic testing, are particularly suitable and are used in numerous different methodological approaches. However, active infrared thermography should also be mentioned here as a surface method, since an increased penetration depth can also be achieved by adjusting the test times. Although there are more recent but less common methods such as ground penetrating radar [261], terahertz [262], or shearography [263], that could be used for testing thick-walled FRP, the aim of this review is to focus on more established NDT procedures.

5.1. Ultrasound

Due to the requirement profiles in the standardised area of quality assurance, ultrasonic testing (UT) has become a standard NDT procedure. While standards often specify the beam angle, test frequencies, and other specifications for certain components, this is currently not the case in the area of FRP. Existing standards and guidelines can only be applied with caution, particularly in the case of very thick-walled FRP laminates. The high number of interfaces in a thick-walled FRP laminate leads to a significant loss of sound energy through reflection and scattering. As a result, the internal attenuation increases significantly, especially at high frequencies. For this reason, frequencies between 0.5 MHz and 5 MHz are usually used in practice, depending on the thickness, the layer structure and the fibre volume content of the FRP test specimen to be tested. Various studies show that glass fibre reinforced polymers up to a thickness of around 50 mm can be tested with a test frequency of 0.5 MHz [264,265].

The proportion of sound energy reflected at an interface depends on the acoustic properties of the neighbouring media. A particularly high proportion of reflected sound energy results at an interface between a solid material like FRP and air, which is why the UT is particularly suitable for detecting defects with air inclusions (voids and delaminations) [266]. This leads to the problem that sound transmission is more difficult with thick-walled FRP, where the pore density is higher than with thin-walled FRP due to the manufacturing challenges [267]. In [268] this effect is utilised to investigate the degree of porosity in 11 mm thick carbon fibre reinforced polymers (CFRP) specimens. The

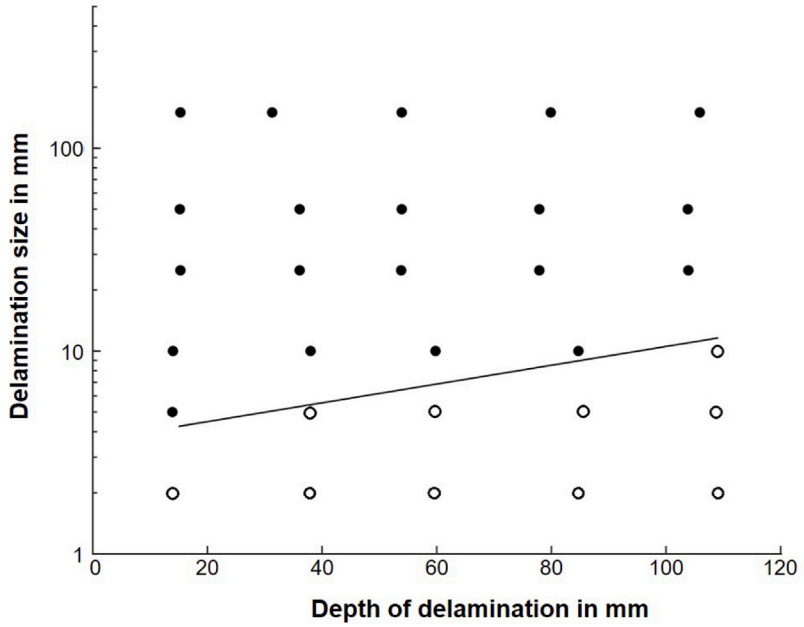

Fig. 11. Diagram showing the detection limit of delaminations at different depths according to [269]. Filled-in dots represent detectable delaminations. The diagonal line represents the detectability limit proposed by the author.

problem of high damping was also analysed in [269] and the detection limit of delaminations of different sizes was determined at a depth of up to approximately 110 mm (see Fig. 11).

In addition to the high attenuation, the high degree of anisotropy of the FRP also poses corresponding challenges in ultrasonic testing. The directional dependence of the sound velocity leads to complex evaluation approaches, particularly in the case of angled scanning, in order to determine the position of defects. However, the characterisation of this anisotropic behaviour also offers the possibility of drawing conclusions about the internal structure of an FRP. Thus, in [270], guided waves are used to investigate the in-plane fibre orientation of a 10.5 mm thick CFRP test specimen. By analysing different modes, it was also possible to carry out a depth-resolved evaluation of the stiffness. The authors in [271] also deal with the problem of increasing fibre waviness in thick-walled FRP. They show a simulative approach in which guided waves are used to perform the localisation and severity assessment of fibre waviness in the laminate plane and undulations in the thickness direction in a 7 mm thick CFRP sheet. Although the experimental proof of this approach is missing here, this work shows the relevance of the subject. Further investigations in [272] show that in thick-walled FRP, the detection probability of defects using conventional evaluation methods decreases due to increased fibre waviness. They found that in a 12 mm thick CFRP with strong fibre waviness, voids with a size of 2 mm can no longer be reliably detected using a conventional B-scan. They developed a method with a transmission setup of two phased array probes, which improves the defect detection significantly and also allows depth-resolved determination of the fibre waviness.

As the signal amplitudes decrease with increasing laminate thickness, reconstruction algorithms can be used to improve the signal-to-noise ratio. For example, [273] presents an approach using the Total Focusing Method (TFM), in which anisotropic sound velocities of an FRP are adjusted. As a result, the signal-to-noise ratio could be improved by around 15 dB up to a defect depth of 16 mm.

As the sound attenuation in thick-walled FRP laminates increases with increasing test frequency [274], there are various studies on the use of air-coupled ultrasound. This is a non-contact testing method in which special transducers adapted to the air are used. In order to achieve a sufficient SNR despite the non-contact application, the probes are operated with a significantly higher energy and at frequencies below the usual UT range, usually in the range of 25–500 kHz. These lower frequencies lead to reduced sound attenuation in the test specimen. This is demonstrated in [264], where the testability of 50 mm thick GFRP laminates is demonstrated at 400 kHz and 120 kHz, with better results obtained at the lower test frequency. In [275], CFRP test specimens with a thickness between 0.7 mm and 50.8 mm were tested at a test frequency of 200 kHz. This paper shows that the amplitude decreases by approximately 80%. In addition, the authors demonstrate the possibility of using thickness resonances through a skilful choice of test frequency, which in their case leads to an increase in signal amplitude of around 50% for a component thickness of 24 mm.

5.2. X-ray inspection and X-ray computed tomography

X-ray testing (RT) is also one of the volume methods of non-destructive testing. Here, an X-ray source is directed at the test specimen and the intensity of the transmitting radiation is recorded using a detector. Different attenuation effects in the test specimen, caused by different materials and radiation lengths, create a contrast in the X-ray image and allow conclusions to be drawn about the internal structure, fibre orientation and the presence of defects such as cracks or delamination. To improve the level of detail in RT, it is important to maximise the contrast of an X-ray image. This is an important detail when testing thick-walled FRP, as the increasing wall thickness of a test specimen leads to an increasing deterioration in contrast. To counteract this, it is particularly important to increase and optimise the tube voltage and tube current for a specific test case [276]. In addition, the use of highly absorbent contrast agents enables a further improvement in defect detection. Two principal approaches can be distinguished: ex-situ penetrant methods for surface-breaking defects and in-situ integrated contrast agents. Ex-situ methods utilise high-atomic-number liquids such as zinc iodide (ZnI_2) to infiltrate surface-breaking cracks, delaminations, and voids. This approach, frequently applied in aerospace composites, substantially improves the detectability of internal damage, including matrix cracks and delamination fronts [277, 278]. In [279] a zinc iodide solution is used to improve the contrast of vertically orientated cracks on 4.1 mm and 6.1 mm thick CFRP test specimens. However, ZnI_2 can alter subsequent damage growth, e.g. by accelerating crack propagation, restricting its use to diagnostic investigations [280]. Furthermore, the penetration depth of all

penetrants in thick-walled specimens is limited [281]. To overcome this problem, in-situ approaches introduce contrast-enhancing agents during composite manufacturing. Early work demonstrated that resin additives or metallic coatings on fibre tows enhance X-ray contrast between fibres, matrix, and voids, enabling improved microstructural segmentation [282]. More recent studies have shown that dispersing hafnium oxide (HfO_2) nanocrystals in the epoxy matrix provides strong volumetric contrast while maintaining processability, allowing reliable detection of microcracks and fibre bundle architecture across the entire laminate [283]. While the method enhances the visibility of internal defects, the associated increase in bulk attenuation amplifies the challenges encountered when inspecting components with substantial wall thickness. Similar to ultrasound, reconstruction approaches enable an optimised presentation of the test results. In the case of RT, computed tomography (CT) analysis enables a significant improvement in the results. For this purpose, several individual images of a rotating test specimen are taken at defined angular increments. Image reconstruction algorithms are used to reconstruct these individual images into a 3D map consisting of volume elements (voxels). Each voxel has a characteristic grey value, which correlates with attenuation coefficients at this point. This method was used to determine the extent of impact damage in a 43.18 mm thick GFRP test specimen [284]. However, it must be noted that the evaluation of volumes such as pores or delaminations depends heavily on the selected threshold value, which determines the grey value from which a voxel is counted as a defect. In [285] it was possible to calculate a fluctuation range of the calculated porosity between 3.8% and 8.3% for different threshold values in a porous CFRP laminate. A further limitation arises from the physical size constraints of most CT systems: thick-walled FRP components often also have large overall dimensions, making them difficult or impossible to scan in their entirety. In such cases, specimen extraction from the original structure may be required, which negates the non-destructive nature of the method. In principle, CT technology offers the possibility of resolving individual fibres in the composite using adapted focal spot sizes and high-resolution detectors. The size of a voxel should not be much larger than 2 µm, depending on the fibre diameter [286,287]which also shows the limitation of such an evaluation. In [287], taking into account the detectors commonly used today, it is stated that the test specimen size is limited to around 6 mm for the resolution of individual fibres. This shows that CT is not a suitable non-destructive testing method for the detection of individual fibres in real FRP components. In order to extend this limit, [288] investigated the use of synchrotron radiation in laminography (SRCL) and compared it with the μCT method. Here, SRCL was used to test a $150 \times 100 \times 4.5$ mm^3 CFRP test plate without the destructive removal of the region of interest required by μCT and an improvement in resolution by a factor of 6 compared to the μCT results was found. Another advantage of the SRCL is that the entire test specimen can be tested. The destructive specimens segmentation required for μCT is no longer necessary.

5.3. Thermography

The great advantage of infrared thermography testing (TT) lies in the non-contact, non-invasive, dry, safe, and fast execution as well as the direct imaging of the test results [260]. In active TT, an external thermal excitation source such as pulsed halogen lamps [289] or lasers [290] is used to heat the specimen's surface. Thermal energy can also be introduced mechanically by ultrasonic excitation or electromagnetically by induction [291]. The advantage is, that the heat is generated directly at the defects, which improves the detection of small defects. After the excitation, the time-dependent temperature of the specimen surface is then recorded, using an infrared camera. Defects like delamination can be localised through locally differing heat dissipation, which can be detected as hot spots in the recorded temperature images. Since similar hotspots can also be caused by the effects of artifacts (e.g. reflections from the environment, air turbulence, inhomogeneous infrared emission coefficient), the more robust phase-sensitive modulation thermography (or lock-in thermography) is widely used.

In theory, it should be easy to answer the question of whether thick-walled FRP can be tested using thermography. With lock-in thermography, the thermal penetration depth μ can be calculated as follows using the modulation frequency f and the thermal diffusivity α of the material.

$$\mu = \sqrt{\frac{\alpha}{\pi f}} \tag{1}$$

With a decreasing test frequency and, as a result, an increasing test period, the penetration depth of the thermal waves and, therefore, the detectability of defects in thick FRPs increases. In reality, the depth resolution of defects is limited by the lateral heat fluxes, that leads to an increasing blurring up to the recognisability of the defect in the obtained test results. As a rule of thumb for every thermography method, a defect can only be detected if the lateral size of the damage corresponds at least to its depth in the test specimen. In [292] the author deals with the theoretical and experimental limit to which depth an air-filled defect with a diameter of 10 mm can be detected in graphite/epoxy composites up to 15 mm thick. Due to the excitation methods used (Flash heating and Square-pulse heating), the results are just below the aforementioned rule of thumb.

As with every NDT method, the challenges in terms of testability of thick specimens are increasing in TT. The authors in [293] failed to carry out successful measurements on a 30 mm thick CFRP component, using flash thermography. They base this on the low thermal energy used for the excitation and the inhomogeneity of the specimen. Despite this, the authors of [294] were able to demonstrate the testability of GFRP laminates up to 30 mm thick using the sun as the excitation source. By extending the excitation and cooling time to at least 10 min, they were able to visualise adhesive flaws between GFRP and the foam core in real wind turbine blades. This method is also described in [295] to detect various defects such as flat bottom holes and bubble wrap inserts up to a depth of 10 mm.

However, it should also be mentioned that there is currently a great research activity into new approaches to undercut the above-mentioned rule of thumb for error detection and to improve the detection sensitivity of TT. One approach is the virtual wave concept, which transfers the thermal wave propagation as a diffusive process into a kind of acoustic wave, which allows the use of reconstruction algorithms known from ultrasound for the post-processing of thermography results [296]. It is shown, that with the virtual wave concept, defects that are smaller than their depth can still be detected using conventional inspection technology. However, since this concept requires solving the inverse problem, which is associated with considerable computational effort, the black-box approach using AI appears to be the more elegant solution for practical applications. Again, initial results show [297] that there is far more information in the test data than is actually exploited by traditional readout methods. Another approach shown by [298] is an adapted excitation, in which the excitation is not homogeneous in space and time. Through a spatial- and temporal-structured heating, the lateral heat flux that distort the response image can be specifically compensated in this way. Using this approach, [299] showed that the spatial resolution in the lock-in thermography can be significantly increased (see Fig. 12). Although this has not yet been demonstrated for thick-walled FRP, there are no fundamental concerns about the transferability of the published algorithms to thick-walled components.

5.4. Acoustic emission

Compared to the other test methods presented here, acoustic emission testing (AT) is a passive test method in which elastic stress waves

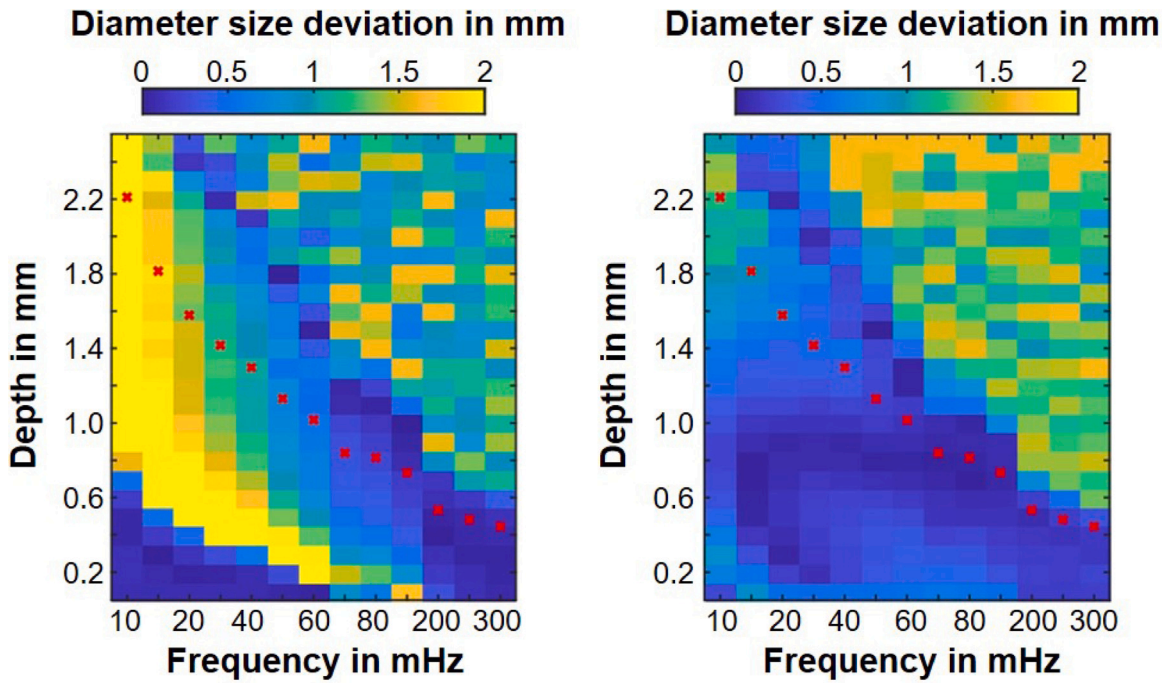

Fig. 12. Simulated frequency–depth images of a 2 mm flat bottom hole for the deviation of the diameter between the actual size and the computed result according to [299]: Left shows the result of a lock-in thermography and right the results of the novel lock-in compensation method.

are registered in the ultrasonic range, which are generated by stress concentrations and crack initiation or propagation caused by an external load. The elastic stress waves can occur in the form of volume, Rayleigh and Lamb waves. Due to the concentric propagation of these waves around a developing defect, it can be detected, classified and located using multiple piezoelectric receivers and by applying reconstruction algorithms to the received signal. The thickness of the test specimen plays a decisive role in these algorithms, as it has a significant influence on the amplitude and phase velocity of the Rayleigh and Lamb modes that are generated. This is of particular importance for the evaluation, as the different modes (symmetrical and asymmetrical) have also a different acoustic attenuation [300]. In addition, [301] shows a dependence of the resulting Lamb modes on the defect depth, with a linear decrease in the amplitude ratio between asymmetric and symmetric Lamb modes with increasing defect depth. A large area of application for the AT is the rotor blade testing of wind turbine blades (WTB). For this application, there are numerous publications dealing with the application, optimisation and improved reconstruction analysis of the AT. For example, the authors in [302] conducted an experimental study on the monitoring of the operating condition of WTBs and found that cracks could be localised at an early stage by adapting evaluation algorithms. Since the complex test setup with several sensors means that a large amount of data is collected over a long period of time, [303] presents a statistical evaluation approach for comparing the quadratic mean values of a measurement with the modal parameters of the WTB. With 200 measurement points and 10 vibration modes considered, the locations for three analysed defect positions could be determined. Similar to conventional ultrasonic testing, non-contact testing is also possible with air-coupled ultrasonics testing. In [304] a test setup with an array of 48 microphones is set up to detect holes and cracks in a WTB.

6. Conclusion

Thick-walled fibre-reinforced polymer (FRP) composites present significant challenges in both manufacturing and in the application of destructive and non-destructive testing methods. While all established manufacturing techniques are, in principle, applicable to the production of thick-walled FRPs, the curing process requires careful adaptation to minimise residual stresses and the associated manufacturing defects. Future research should prioritise the detailed analysis and simulation of curing behaviour, with particular emphasis on the development of validated models to accurately predict residual stress formation. Real-time process monitoring is essential to provide the data necessary for validating process simulations and accurately modelling curing behaviour.

The quasi-static mechanical behaviour of thick-walled FRPs has been extensively investigated. Compared to their thin-walled counterparts, thick-walled composites consistently exhibit reduced strength across all loading conditions. Fatigue testing further reveals a decrease in service life with increasing wall thickness. Future investigations should focus more intently on self-heating phenomena during cyclic loading, which remain insufficiently understood. Moreover, the current understanding of the relationship between laminate thickness and impact performance — especially under high and hypervelocity impacts — is limited and warrants further study.

The numerical analysis of size and thickness effects in FRPs has gained increasing relevance, because of its potential to optimise mechanical properties and structural performance. Key research areas include finite element modelling, parametric studies of thickness effects, and size-dependent fracture mechanics. Recent efforts have begun to integrate manufacturing-induced, thickness-dependent defects into numerical simulations. Initial numeric studies demonstrate that accounting for nesting effects is critical for accurately predicting damage initiation and stiffness degradation. Experimental findings suggest that out-of-plane compressive loading can significantly alter failure mechanisms, thereby underlining the importance of detailed multi-scale characterisation to capture these complex interactions. In this regard, in-situ computed tomography (CT) has proven effective for identifying nesting behaviour in textile reinforcements using advanced imaging techniques. Collectively, these findings highlight the limitations of conventional strength-based or linear elastic fracture mechanics approaches in capturing the quasi-brittle behaviour of thick-walled FRPs, and underscore the need for size-sensitive modelling strategies.

Given the inherent difficulties associated with the manufacturing and mechanical testing of thick-walled laminates, non-destructive testing (NDT) methods represent a valuable tool for characterising these materials. Various NDT techniques are suitable for assessing manufacturing quality, localising internal defects, and evaluating mechanical properties. While no universal thickness limit exists across all NDT methods, ultrasonic and X-ray inspection have shown particular promise in detecting damage deep within the laminate with high resolution. However, the applicability of computed tomography remains constrained by the size of the component under investigation.

In conclusion, despite considerable advances over the past three decades, the understanding of thick-walled FRP composites remains incomplete. Future research should aim to develop models and methodologies that capture the complex influence of size effects, thereby contributing to a more holistic understanding of the mechanical behaviour of fibre-reinforced polymer composites.

CRediT authorship contribution statement

Richard Protz: Writing – original draft, Visualization, Methodology, Conceptualization. **Eckart Kunze:** Writing – original draft, Methodology, Formal analysis. **Tim Luplow:** Writing – original draft, Visualization, Investigation. **Linus Littner:** Writing – original draft, Visualization, Investigation. **Jonas Drummer:** Writing – original draft, Visualization, Investigation. **Sebastian Heimbs:** Writing – review & editing, Supervision, Project administration, Funding acquisition. **Marc Kreutzbruck:** Writing – review & editing, Supervision, Project administration, Funding acquisition. **Bodo Fiedler:** Writing – review & editing, Supervision, Project administration, Funding acquisition. **Maik Gude:** Writing – review & editing, Supervision, Project administration, Funding acquisition.

Declaration of competing interest

The authors declare that they have no known competing financial interests or personal relationships that could have appeared to influence the work reported in this paper.

Acknowledgements

This review paper has been created as part of the PAK 988 package project with the sub-projects 428328210, 428326921, 428323347 and 428324840 of the German Research Foundation (DFG). We are grateful for the financial support.

Data availability

Data will be made available on request.

References

[1] Luplow T, Protz R, Littner L, Drummer J, Kunze E, Heimbs S, Horst P, Gude M, Kreutzbruck M, Fiedler B. Herausforderungen dickwandiger, duroplastischer Faser-Kunststoff-Verbunde in der Herstellung sowie mechanischenund zerstörungsfreien Prüfung — Ein Review. Kunststofftechnik 2023;2(19):73–117. http://dx.doi.org/10.3139/O999.02022023.

[2] de Vries H. Development of a main landing gear attachment fitting using composite material and resin transfer moulding. 2009, URL: https://api.semanticscholar.org/CorpusID:136950504.

[3] Viscardi M, Arena M, Cerreta P, Iaccarino P, Imparato SI. Manufacturing and validation of a novel composite component for aircraft main landing gear bay. J Mater Eng Perform 2019;28(6):3292–300. http://dx.doi.org/10.1007/s11665-019-04106-y.

[4] Chen X. Fracture of wind turbine blades in operation—Part I: A comprehensive forensic investigation. Wind Energy 21(11):1046–63. http://dx.doi.org/10.1002/we.2212, URL: https://onlinelibrary.wiley.com/doi/abs/10.1002/we.2212.

[5] Jensen FM, Puri AS, Dear JP, Branner K, Morris A. Investigating the impact of non-linear geometrical effects on wind turbine blades—Part 1: Current status of design and test methods and future challenges in design optimization. Wind Energy 14(2):239–54. http://dx.doi.org/10.1002/we.415, URL: https://onlinelibrary.wiley.com/doi/abs/10.1002/we.415.

[6] Finnegan W, Allen R, Glennon C, Maguire J, Flanagan M, Flanagan T. Manufacture of High-Performance tidal turbine blades using advanced composite manufacturing technologies. Appl Compos Mater 2021;28(6):2061–86. http://dx.doi.org/10.1007/s10443-021-09967-y.

[7] Nie Y, Liu Q, Xiang Z, Zhong S, Huang X. Performance and modification mechanism of recycled glass fiber of wind turbine blades and SBS Composite-Modified asphalt. Appl Sci 2023;13(10). http://dx.doi.org/10.3390/app13106335, URL: https://www.mdpi.com/2076-3417/13/10/6335.

[8] Rivard E, Trudeau M, Zaghib K. Hydrogen storage for mobility: A review. Materials 2019;12(12). http://dx.doi.org/10.3390/ma12121973, URL: https://www.mdpi.com/1996-1944/12/12/1973.

[9] Fang H, Wang D. Simulation analysis of delamination damage for the Thick-Walled Composite-Overwrapped pressure vessels. Materials 2022;15(19). http://dx.doi.org/10.3390/ma15196880, URL: https://www.mdpi.com/1996-1944/15/19/6880.

[10] Zheng H, Zeng X, Zhang J, Sun H. The application of carbon fiber composites in cryotank. In: Ares AE, editor. Solidification. Rijeka: IntechOpen; 2018, http://dx.doi.org/10.5772/intechopen.73127.

[11] Grogan D. Damage and permeability in linerless composite cryogenic tanks (Ph.D. thesis), 2015.

[12] Liu N, Ma B, Liu F, Huang W, Xu B, Qu L, Yang Y. Progress in research on composite cryogenic propellant tank for large aerospace vehicles. Compos A: Appl Sci Manuf 2021;143:106297. http://dx.doi.org/10.1016/j.compositesa.2021.106297, URL: https://www.sciencedirect.com/science/article/pii/S1359835X21000270.

[13] Rubino F, Nisticò A, Tucci F, Carlone P. Marine application of fiber reinforced composites: A review. J Mar Sci Eng 2020;8(1). http://dx.doi.org/10.3390/jmse8010026, URL: https://www.mdpi.com/2077-1312/8/1/26.

[14] Mouritz A, Gellert E, Burchill P, Challis K. Review of advanced composite structures for naval ships and submarines. Compos Struct 2001;53(1):21–42. http://dx.doi.org/10.1016/S0263-8223(00)00175-6, URL: https://www.sciencedirect.com/science/article/pii/S0263822300001756.

[15] Islami DP, Muzaqih AF, Adiputra R, Prabowo AR, Firdaus N, Ehlers S, Braun M, Jurkovič M, Smaradhana DF, Carvalho H. Structural design parameters of laminated composites for marine applications: Milestone study and extended review on current technology and engineering. Results Eng 2024;24:103195. http://dx.doi.org/10.1016/j.rineng.2024.103195, URL: https://www.sciencedirect.com/science/article/pii/S2590123024014506.

[16] John M, Nama S, D'Antrassi N, Wuestenhagen S, Krombholz A, Schlimper R. Simulation of a prepreg press process using ANSYS Composite Cure Simulation (ACCS). 2017.

[17] Knippers J, Koslowski V, Oppe M. Faserverbundwerkstoffe im bauwesen. In: Stahlbau kalender 2020. John Wiley & Sons, Ltd; 2020, p. 611–70. http://dx.doi.org/10.1002/9783433610053.ch9, URL: https://onlinelibrary.wiley.com/doi/abs/10.1002/9783433610053.ch9.

[18] Qureshi J. A review of fibre reinforced polymer bridges. Fibers 2023;11(5). http://dx.doi.org/10.3390/fib11050040, URL: https://www.mdpi.com/2079-6439/11/5/40.

[19] Wang T, Menshykov O, Menshykova M, Guz IA. Modelling and optimal design of Thick-Walled composite pipes under In-Service conditions. IOP Conf Ser: Mater Sci Eng 2020;936(1):012046. http://dx.doi.org/10.1088/1757-899X/936/1/012046.

[20] Igor A. Guz MM, Paik JK. Thick-walled composite tubes for offshore applications: an example of stress and failure analysis for filament-wound multi-layered pipes. Ships Offshore Struct 2017;12(3):304–22. http://dx.doi.org/10.1080/17445302.2015.1067019.

[21] Wei D, An C, Wu C, Duan M, Estefen SF. Torsional structural behavior of composite rubber hose for offshore applications. Appl Ocean Res 2022;128:103333. http://dx.doi.org/10.1016/j.apor.2022.103333, URL: https://www.sciencedirect.com/science/article/pii/S0141118722002656.

[22] Lee J, Soutis C. Thickness effect on the compressive strength of T800/924C carbon fibre-epoxy laminates. Compos A: Appl Sci Manuf 2005;36(2):213–27. http://dx.doi.org/10.1016/j.compositesa.2004.06.010.

[23] Gao Y, Zhu S, Ding H, Song X, Hu H, Wang H, Ke Y. Thickness variation effect on compressive properties of ultra-thick CFRP laminates. Int J Mech Sci 2023;253:108390. http://dx.doi.org/10.1016/j.ijmecsci.2023.108390, URL: https://www.sciencedirect.com/science/article/pii/S0020740323002928.

[24] Wisnom M. Size effects in the testing of fibre-composite materials. Compos Sci Technol 1999;59(13):1937–57. http://dx.doi.org/10.1016/S0266-3538(99)00053-6, URL: https://www.sciencedirect.com/science/article/pii/S0266353899000536.

[25] Balvers J, Bersee H, Beukers A, Jansen K. Determination of cure dependent properties for curing simulation of thick-walled composites. In: 49th AIAA/aSME/ASCE/AHS/aSC structures, structural dynamics, and materials conference, 16th AIAA/aSME/AHS adaptive structures conference, 10th AIAA

non-deterministic approaches conference, 9th AIAA gossamer spacecraft forum, 4th AIAA multidisciplinary design optimization specialists conference. 2006, p. 2035.
[26] Nsengiyumva W, Zhong S, Lin J, Zhang Q, Zhong J, Huang Y. Advances, limitations and prospects of nondestructive testing and evaluation of thick composites and sandwich structures: A state-of-the-art review. Compos Struct 2021;256:112951.
[27] Kim C, White SR. Thick-walled composite beam theory including 3-D elastic effects and torsional warping. Int J Solids Struct 1997;34(31–32):4237–59.
[28] Zahlen P. Beitrag zur kostengünstigen industriellen fertigung von haupttragenden CFK-Groß komponenten der kommerziellen luftfahrt mittels Kernverbundbauweise in harzinfusionstechnologie (Band 6). Logos Verlag Berlin GmbH; 2013.
[29] Ruiz E, Trochu F. Numerical analysis of cure temperature and internal stresses in thin and thick RTM parts. Compos A: Appl Sci Manuf 2005;36(6):806–26. http://dx.doi.org/10.1016/j.compositesa.2004.10.021.
[30] Schubel PM, Luo JJ, Daniel IM. Through-thickness characterization of thick composite laminates. In: SEM annual conference and exposition on experimental and applied mechanics. 2006, p. 1793–800.
[31] Dmitriev O, Mischenko S. Optimization of curing cycles for thick-wall products of the polymeric composite materials. Adv Compos Mater-Ecodesign Anal 2011;7:141–60.
[32] Esposito L, Sorrentino L, Penta F, Bellini C. Effect of curing overheating on interlaminar shear strength and its modelling in thick FRP laminates. Int J Adv Manuf Technol 2016;87:2213–20.
[33] Altmann A, Taubert R, Mandel U, Hinterhoelzl R, Drechsler K. A continuum damage model to predict the influence of ply waviness on stiffness and strength in ultra-thick unidirectional Fiber-reinforced Plastics. J Compos Mater 2016;50(20):2739–55. http://dx.doi.org/10.1177/0021998315612536.
[34] Zimmermann K, Zenkert D, Siemetzki M. Testing and analysis of ultra thick composites. Compos B: Eng 2010;41(4):326–36. http://dx.doi.org/10.1016/j.compositesb.2009.12.004.
[35] Struzziero G, Teuwen JJE. Residual stresses generation in Ultra-Thick components for wind turbine blades. Procedia CIRP 2019;85:8–12. http://dx.doi.org/10.1016/j.procir.2019.09.002.
[36] Bogetti TA, Gillespie Jr. JW. Two-dimensional cure simulation of thick thermosetting composites. J Compos Mater 1991;25(3):239–73.
[37] Broughton W. Thick composites. 2008.
[38] Potter K, Khan B, Wisnom M, Bell T, Stevens J. Variability, fibre waviness and misalignment in the determination of the properties of composite materials and structures. Compos A: Appl Sci Manuf 2008;39(9):1343–54. http://dx.doi.org/10.1016/j.compositesa.2008.04.016.
[39] Kunze E, Galkin S, Böhm R, Gude M, Kärger L. The impact of draping effects on the stiffness and failure behavior of unidirectional Non-Crimp fabric fiber reinforced composites. Mater (Basel Switz) 2020;13(13). http://dx.doi.org/10.3390/ma13132959.
[40] Thor M, Sause MGR, Hinterhoelzl R. Mechanisms of origin and classification of out-of-plane fiber waviness in composite materials—a review. J Compos Sci 2020;4(3):130. http://dx.doi.org/10.3390/jcs4030130.
[41] Olivier P, Cavarero M. Comparison between longitudinal tensile characteristics of thin and thick thermoset composite laminates: influence of curing conditions. Comput Struct 2000;76(1–3):125–37. http://dx.doi.org/10.1016/S0045-7949(99)00161-3.
[42] Twardowski TE, Lin SE, Geil PH. Curing in thick composite laminates: Experiment and simulation. J Compos Mater 1993;27(3):216–50. http://dx.doi.org/10.1177/002199839302700301.
[43] Broughton W. Thick composites. 2001.
[44] Zhang W, Xu Y, Hui X, Zhang W. A Multi-Dwell temperature profile design for the cure of thick CFRP composite laminates. Int J Adv Manuf Technol 2021;117(3):1133–46. http://dx.doi.org/10.1007/s00170-021-07765-1.
[45] Sun X, Cook L, Belnoue JP, Tifkitsis KI, Kratz J, Skordos AA. Manufacturing thick laminates using a layer by layer curing approach. Compos A: Appl Sci Manuf 2024;187:108489.
[46] Möllers H, Schmidt C, Steuernagel L, Meiners D. Simulative cure optimisation of thick and ultra-thick laminates using multiple epoxy resin systems. In: SAMPE europe conference & exhibition 2024; belfast, united kingdom. 2024.
[47] Zhang B, Li Y, Liu S, Shen Y, Hao X. Layered self-resistance electric heating to cure thick carbon fiber reinforced epoxy laminates. Polym Compos 2021;42(5):2469–83.
[48] Thostenson E, Chou T-W. Microwave processing: fundamentals and applications. Compos A: Appl Sci Manuf 1999;30(9):1055–71. http://dx.doi.org/10.1016/S1359-835X(99)00020-2, URL: https://www.sciencedirect.com/science/article/pii/S1359835X99000202.
[49] Thostenson ET, Chou T-W. Microwave and conventional curing of thick-section thermoset composite laminates: experiment and simulation. Polym Compos 2001;22(2):197–212.
[50] Yuksel O, Baran I, Ersoy N, Akkerman R. Investigation of transverse residual stresses in a thick pultruded composite using digital image correlation with hole drilling. Compos Struct 2019;223:110954. http://dx.doi.org/10.1016/j.compstruct.2019.110954.
[51] Gil A. Manufacturing of thick-walled composites. 2010.
[52] Timms J, Bickerton S, Kelly P. Laminate thickness and resin pressure evolution during axisymmetric liquid composite moulding with flexible tooling. Compos A: Appl Sci Manuf 2012;43(4):621–30.
[53] Zhang L, Wang X, Pei J, Zhou Y. Review of automated fibre placement and its prospects for advanced composites. J Mater Sci 2020;55(17):7121–55.
[54] Mohan RV, Ngo N, Tamma K. Three-dimensional resin transfer molding: Isothermal process modeling and explicit tracking of moving fronts for thick geometrically complex composites manufacturing applications-Part 1. Numer Heat Transf: A: Appl 1999;35(8):815–38.
[55] Matyjaszewski K, Möller M. Polymer science: a comprehensive reference. 2012, (No Title).
[56] Saouab A, Bréard J, Lory P, Gardarein B, Bouquet G. Injection simulations of thick composite parts manufactured by the RTM process. Compos Sci Technol 2001;61(3):445–51.
[57] Ali M, Umer R, Khan K, Cantwell W. Application of X-ray computed tomography for the virtual permeability prediction of fiber reinforcements for liquid composite molding processes: A review. Compos Sci Technol 2019;184:107828.
[58] Yousaf Z, Withers P, Potluri P. Compaction, nesting and image based permeability analysis of multi-layer dry preforms by computed tomography (CT). Compos Struct 2021;263:113676.
[59] Trochu F, Ruiz E, Achim V, Soukane S. Advanced numerical simulation of liquid composite molding for process analysis and optimization. Compos A: Appl Sci Manuf 2006;37(6):890–902.
[60] Li Y, Zhang Z, Li M, Gu Y. Numerical simulation of flow and compaction during the cure of laminated composites. J Reinf Plast Compos 2007;26(3):251–68.
[61] Maguire JM, Sharp ND, Pipes RB, Brádaigh CMÓ. Advanced process simulations for thick-section epoxy powder composite structures. Compos A: Appl Sci Manuf 2022;161:107073.
[62] Centea T, Grunenfelder LK, Nutt SR. A review of out-of-autoclave prepregs–material properties, process phenomena, and manufacturing considerations. Compos A: Appl Sci Manuf 2015;70:132–54.
[63] Hojjati M, Hoa S. Curing simulation of thick thermosetting composites. Compos Manuf 1994;5(3):159–69.
[64] Yan X. Finite element simulation of cure of thick composite: formulations and validation verification. J Reinf Plast Compos 2008;27(4):339–55.
[65] Konstantopoulos S, Hueber C, Antoniadis I, Summerscales J, Schledjewski R. Liquid composite molding reproducibility in real-world production of fiber reinforced polymeric composites: a review of challenges and solutions. Adv Manuf: Polym Compos Sci 2019;5(3):85–99. http://dx.doi.org/10.1080/20550340.2019.1635778.
[66] Galkin S, Kunze E, Kärger L, Böhm R, Gude M. Experimental and numerical determination of the local fiber volume content of unidirectional non-crimp fabrics with forming effects. J Compos Sci 2019;3(1):19. http://dx.doi.org/10.3390/jcs3010019.
[67] Gruhl A. Beitrag zur beanspruchungsgerechten Gestaltung und technologischen umsetzung neuartiger Flechtmuster für Faserverbundstrukturen. 2019.
[68] Gruhl A, Böhm R, Gude M. Faserverbundbauteile auf basis neuartiger flechtmuster. Light Des 2016;9(2):38–43. http://dx.doi.org/10.1007/s35725-016-0007-y.
[69] Khan ZM, Adams DO, Anas S. The influence of multiple nested layer waviness on the compression strength of double nested wave formations in a carbon fiber composite laminate. Mech Compos Mater 2016;51(6):751–60. http://dx.doi.org/10.1007/s11029-016-9546-7.
[70] Gardiner G. Airbus A350 update: BRaF & FPP. CompositesWorld 2012. URL: https://www.compositesworld.com/articles/airbus-a350-update-braf-fpp.
[71] Mishnaevsky L, Branner K, Petersen HN, Beauson J, McGugan M, Sørensen BF. Materials for wind turbine blades: An overview. Mater (Basel Switz) 2017;10(11). http://dx.doi.org/10.3390/ma10111285.
[72] Stewart R. Wind turbine blade production - new products keep pace as scale increases. Reinf Plast 2012;56(1):18–25. http://dx.doi.org/10.1016/S0034-3617(12)70033-4.
[73] Czichon S, Zimmermann K, Middendorf P, Vogler M, Rolfes R. Three-dimensional stress and progressive failure analysis of ultra thick laminates and experimental validation. Compos Struct 2011;93(5):1394–403. http://dx.doi.org/10.1016/j.compstruct.2010.11.009.
[74] Neitzel M. Handbuch verbundwerkstoffe. In: Neitzel M, Mitschang P, Breuer U, editors. Handbuch verbundwerkstoffe. Carl Hanser Verlag GmbH & Co. KG; 2014, p. I–XXI.
[75] Siebenpfeiffer W. Leichtbau-technologien im automobilbau. Springer; 2014.
[76] Vita A, Castorani V, Germani M. Manufacturing, process simulation and mechanical tests of a thick component produced by compression-RTM process. In: Eccm18-18th European conference on composite materials. 2018, p. 24–8.
[77] Rosenberg P. Entwicklung einer RTM prozessvariante zur kavitätsdruckgeregelten herstellung von faserverbundstrukturbauteilen (Ph.D. thesis), Karlsruher Institut für Technologie (KIT); 2018.
[78] Chaudhari R. Characterization of high-pressure resin transfer molding process variants for manufacturing high-performance composites. 2014, http://dx.doi.org/10.24406/PUBLICA-FHG-280078, ????.
[79] Barcenas Gomez L. Residual stresses during liquid moulding of composites with highly reactive thermosets. 2024.

[80] Taddei F, Struzziero G, Michaud V. Mitigation of infusion and cure-induced defects for thick thermosetting composites: Current challenges and future trends. Polym Compos 2025.

[81] Kempner EA, Hahn H. Effect of radial stress relaxation on fibre stress in filament winding of thick composites. Compos Manuf 1995;6(2):67–77. http://dx.doi.org/10.1016/0956-7143(95)99646-A.

[82] Cohen D. Influence of filament winding parameters on composite vessel quality and strength. Compos A: Appl Sci Manuf 1997;28(12):1035–47. http://dx.doi.org/10.1016/S1359-835X(97)00073-0.

[83] Miao Y, Liu X, Geng Y, Zhang M. Numerical simulation research of winding tension system based on hoop residual stress of thick-walled composite. In: Journal of physics: conference series. vol. 2783, IOP Publishing; 2024, 012048.

[84] Ekuase OA, Anjum N, Eze VO, Okoli OI. A review on the Out-of-Autoclave process for composite manufacturing. J Compos Sci 2022;6(6):172. http://dx.doi.org/10.3390/jcs6060172.

[85] Martulli LM, Creemers T, Schöberl E, Hale N, Kerschbaum M, Lomov SV, Swolfs Y. A thick-walled sheet moulding compound automotive component: Manufacturing and performance. Compos A: Appl Sci Manuf 2020;128:105688. http://dx.doi.org/10.1016/j.compositesa.2019.105688.

[86] Netzel C, Hoffmann D, Battley M, Hubert P, Bickerton S. Effects of environmental conditions on uncured prepreg characteristics and their effects on defect generation during autoclave processing. Compos A: Appl Sci Manuf 2021;151:106636.

[87] Guo Z-S, Du S, Zhang B. Temperature field of thick thermoset composite laminates during cure process. Compos Sci Technol 2005;65(3–4):517–23.

[88] Li Y, Chen G, Ge J, Liu K, Liang J. Modeling of curing process and residual stress analysis of thick-section thermosetting composites. Acta Mech Sin 2026;42(1):424411.

[89] Antonucci V, Giordano M, Imparato SI, Nicolais L. Autoclave manufacturing of thick composites. Polym Compos 2002;23(5):902–10.

[90] Netzel C, Mordasini A, Schubert J, Allen T, Battley M, Hickey C, Hubert P, Bickerton S. An experimental study of defect evolution in corners by autoclave processing of prepreg material. Compos A: Appl Sci Manuf 2021;144:106348.

[91] Gongadze E, Dighton C, Nash G, Moss M, Hemingway B, Belnoue JP-H, Hallett SR. Thickness control of autoclave-molded composite laminates. J Manuf Sci Eng 2023;145(9):091006.

[92] Ekuase OA, Anjum N, Eze VO, Okoli OI. A review on the out-of-autoclave process for composite manufacturing. J Compos Sci 2022;6(6):172.

[93] Smith IL, McCarthy ED, Thies PR, Oterkus S, Obande W. Experimental investigation of thickness effects in the manufacture of thick-section composite structures using liquid thermoplastic resin. Adv Manuf: Polym Compos Sci 2025;11(1):2521570.

[94] Maguire JM, Simacek P, Advani SG, Brádaigh CMÓ. Novel epoxy powder for manufacturing thick-section composite parts under vacuum-bag-only conditions. Part I: Through-thickness process modelling. Compos A: Appl Sci Manuf 2020;136:105969.

[95] Ha SK, Jeong JY. Effects of winding angles on through-thickness properties and residual strains of thick filament wound composite rings. Compos Sci Technol 2005;65(1):27–35. http://dx.doi.org/10.1016/j.compscitech.2004.05.019.

[96] Azeem M, Ya HH, Alam MA, Kumar M, Stabla P, Smolnicki M, Gemi L, Khan R, Ahmed T, Ma Q, Sadique MR, Mokhtar AA, Mustapha M. Application of filament winding technology in composite pressure vessels and challenges: A review. J Energy Storage 2022;49:103468. http://dx.doi.org/10.1016/j.est.2021.103468.

[97] Volk M, Yuksel O, Baran I, Hattel JH, Spangenberg J, Sandberg M. Cost-efficient, automated, and sustainable composite profile manufacture: A review of the state of the art, innovations, and future of pultrusion technologies. Compos B: Eng 2022;246:110135. http://dx.doi.org/10.1016/j.compositesb.2022.110135.

[98] Yuksel O, Sandberg M, Hattel JH, Akkerman R, Baran I. Mesoscale process modeling of a thick pultruded composite with variability in fiber volume fraction. Mater (Basel Switz) 2021;14(13). http://dx.doi.org/10.3390/ma14133763.

[99] Yousaf Z, Potluri P, Withers P. Influence of tow architecture on compaction and nesting in textile preforms. Appl Compos Mater 2017;24(2):337–50.

[100] Thompson AJ, McFarlane JR, Belnoue JP-H, Hallett SR. Numerical modelling of compaction induced defects in thick 2D textile composites. Mater Des 2020;196:109088.

[101] Chen B, Chou T-W. Compaction of woven-fabric preforms: nesting and multi-layer deformation. Compos Sci Technol 2000;60(12–13):2223–31.

[102] Shin DD, Hahn HT. Compaction of thick composites: simulation and experiment. Polym Compos 2004;25(1):49–59.

[103] Vinot M, Holzapfel M, Jemmali R. Numerical investigation of carbon braided composites at the mesoscale: using computer tomography as a validation tool. In: 10th European LS-DYNA conference, würzburg, Germany. 2015.

[104] Bodaghi M, Lomov S, Simacek P, Correia N, Advani S. On the variability of permeability induced by reinforcement distortions and dual scale flow in liquid composite moulding: A review. Compos A: Appl Sci Manuf 2019;120:188–210.

[105] Pedneau ER, Wang SS. Three-Dimensional permeability of Thick-Section glass fabric reinforced polymer composite by Vacuum-Assisted resin infusion molding. J Manuf Sci Eng 2022;144(7):071013.

[106] Poodts E, Minak G, Mazzocchetti L, Giorgini L. Fabrication, process simulation and testing of a thick CFRP component using the RTM process. Compos B: Eng 2014;56:673–80.

[107] Liu G, Luo C, Zhang D, Li X, Qu P, Sun X, Jia Y, Yi X. Mechanical performance and failure mechanism of thick-walled composite connecting rods fabricated by resin transfer molding technique. Appl Compos Mater 2015;22:423–36.

[108] Bodaghi M, Simacek P, Advani SG, Correia NC. A model for fibre washout during high injection pressure resin transfer moulding. J Reinf Plast Compos 2018;37(13):865–76.

[109] Yenilmez B, Senan M, Sozer EM. Variation of part thickness and compaction pressure in vacuum infusion process. Compos Sci Technol 2009;69(11–12):1710–9.

[110] Kim D, Centea T, Nutt S. In-situ cure monitoring of an out-of-autoclave prepreg: Effects of out-time on viscosity, gelation and vitrification. Compos Sci Technol 2014;102:132–8.

[111] Giorgini L, Mazzocchetti L, Benelli T, Minak G, Poodts E, Dolcini E. Kinetics and modeling of curing behavior for two different prepregs based on the same epoxy precursor: A case study for the industrial design of thick composites. Polym Compos 2013;34(9):1506–14.

[112] Gao Y, Ye J, Yuan Z, Ling Z, Zhou Y, Lin Z, Dong J, Wang H, Peng H-X. Optimization strategy for curing ultra-thick composite laminates based on multi-objective genetic algorithm. Compos Commun 2022;31:101115.

[113] Michaud D, Beris A, Dhurjati P. Thick-sectioned RTM composite manufacturing: part I–in situ cure model parameter identification and sensing. J Compos Mater 2002;36(10):1175–200.

[114] Ren M, Wang Q, Cong J, Chang X. Study of one-dimensional cure simulation applicable conditions for thick laminates and its comparison with three-dimensional simulation. Sci Eng Compos Mater 2018;25(6):1197–204.

[115] Park HC, Lee SW. Cure simulation of thick composite structures using the finite element method. J Compos Mater 2001;35(3):188–201.

[116] Konstantopoulos S, Fauster E, Schledjewski R. Monitoring the production of FRP composites: A review of in-line sensing methods. Express Polym Lett 2014;8(11). http://dx.doi.org/10.3144/expresspolymlett.2014.84.

[117] Kim R-W, Kim C-M, Hwang K-H, Kim S-R. Embedded based Real-Time monitoring in the High-Pressure resin transfer molding process for CFRP. Appl Sci 2019;9:1795. http://dx.doi.org/10.3390/app9091795.

[118] Littner L, Protz R, Kunze E, Bernhardt Y, Kreutzbruck M, Gude M. Flow front monitoring in high-pressure resin transfer molding using phased array ultrasonic testing to optimize mold filling simulations. Materials 2024;17(1). URL: https://www.mdpi.com/1996-1944/17/1/207.

[119] Yenilmez B, Sozer EM. A grid of dielectric sensors to monitor mold filling and resin cure in resin transfer molding. Compos A: Appl Sci Manuf 2009;40(4):476–89. http://dx.doi.org/10.1016/j.compositesa.2009.01.014.

[120] Zhang H, Guo P, Jin K. Design of an HP-RTM flow monitoring system based on embedded capacitive sensors. 2025, p. 91–5. http://dx.doi.org/10.1109/ICSI64877.2025.11009490.

[121] Schmachtenberg E, zur Schulte Heide J, Töpker J. Application of ultrasonics for the process control of Resin Transfer Moulding (RTM). Polym Test 2005;24(3):330–8. http://dx.doi.org/10.1016/j.polymertesting.2004.11.002.

[122] Rath M, Döring J, Stark W, Hinrichsen G. Process monitoring of moulding compounds by ultrasonic measurements in a compression mould. NDT E Int 2000;33(2):123–30. http://dx.doi.org/10.1016/S0963-8695(99)00029-8.

[123] Drinkwater BW, Wilcox PD. Ultrasonic arrays for non-destructive evaluation: A review. NDT E Int 2006;39(7):525–41. http://dx.doi.org/10.1016/j.ndteint.2006.03.006.

[124] Stöven T, Weyrauch F, Mitschang P, Neitzel M. Continuous monitoring of three-dimensional resin flow through a fibre preform. Compos A: Appl Sci Manuf 2003;34(6):475–80. http://dx.doi.org/10.1016/S1359-835X(03)00059-9.

[125] Protz R. Zum einfluss von defekten auf das dehnratenabhängige werkstoffverhalten von faser-kunststoff-verbunden (Ph.D. thesis), Technische Universität Dresden; 2021.

[126] O'Brien TK, Chawan AD, DeMarco K, Paris I. Influence of specimen preparation and specimen size on composite transverse tensile strength and scatter. 2001.

[127] Griffin DA. Windpact turbine design scaling Studies Technical Area 1-Composite Blades for 80- to 120-Meter rotor. 2001, URL: https://www.osti.gov/biblio/783406.

[128] Gamstedt EK, Andersen SI. Fatigue degradation and failure of rotating composite structures - Materials characterisation and underlying mechanisms. Roskilde (Denmark): Risoe National Lab., Materials Research Dept.; 2001.

[129] Krämer ET, Grouve WJB, Koussios S, Warnet LL, Akkerman R. Real-time observation of waviness formation during C/PEEK consolidation. Compos A: Appl Sci Manuf 2020;133:105872. http://dx.doi.org/10.1016/j.compositesa.2020.105872.

[130] Belnoue J-H, Nixon-Pearson OJ, Thompson AJ, Ivanov DS, Potter KD, Hallett SR. Consolidation-driven defect generation in thick composite parts. J Manuf Sci Eng 2018;140(7). http://dx.doi.org/10.1115/1.4039555.

[131] Melin LG, Levin K, Nilsson S, Palmer SJ, Rae P. A study of the displacement field around embedded fibre optic sensors. Compos A: Appl Sci Manuf 1999;30(11):1267–75. http://dx.doi.org/10.1016/S1359-835X(99)00036-6.

[132] Barfuss D, Garthaus C, Gude M. Advanced waviness modelling of thermoplastic tape braids. In: Proceedings ICCM20. 2015, p. 19–24.

[133] Lomov SV, Verpoest I, Peeters T, Roose D, Zako M. Nesting in textile laminates: geometrical modelling of the laminate. Compos Sci Technol 2003;63(7):993–1007. http://dx.doi.org/10.1016/S0266-3538(02)00318-4.

[134] Böhm R, Kunze E, Geller S, Gude M. Experimental analysis of draping process generated material imperfections in textile preforms. In: ECCM18 - 18th European conference on composite materials. 2018.

[135] Bodaghi M, Simacek P, Advani SG, Correia NC. A model for fibre washout during high injection pressure resin transfer moulding. J Reinf Plast Compos 2018;37(13):865–76. http://dx.doi.org/10.1177/0731684418765960.

[136] Hautefeuille A, Comas-Cardona S, Binetruy C. Consolidation and compression of deformable impregnated fibrous reinforcements: Experimental study and modeling of flow-induced deformations. Compos A: Appl Sci Manuf 2020;131:105768.

[137] Bodaghi M, Cristóvão C, Gomes R, Correia NC. Experimental characterization of voids in high fibre volume fraction composites processed by high injection pressure RTM. Compos A: Appl Sci Manuf 2016;82:88–99.

[138] Pierce RS, Falzon BG. Simulating resin infusion through textile reinforcement materials for the manufacture of complex composite structures. Engineering 2017;3(5):596–607. http://dx.doi.org/10.1016/J.ENG.2017.04.006.

[139] Rutt M, Lekakou C, Smith PA, Sordon A, Santoni C, Meeks G, Hamerton I. Methods for process-related resin selection and optimisation in high-pressure resin transfer moulding. Mater Sci Technol 2019;35(3):327–35. http://dx.doi.org/10.1080/02670836.2018.1557916.

[140] Chen Z, Peng L, Xiao Z. Experimental characterization and numerical simulation of voids in CFRP components processed by HP-RTM. Materials 2022;15(15). http://dx.doi.org/10.3390/ma15155249, URL: https://www.mdpi.com/1996-1944/15/15/5249.

[141] Padaki NV, Alagirusamy R, Deopura BL, Fangueiro R. Compression and permeability properties of multiaxial warp-knit preforms. J Text Inst 2008;99(4):287–94. http://dx.doi.org/10.1080/00405000701414733.

[142] Becker D. Transversales imprägnierverhalten textiler verstärkungsstrukturen für faser-kunststoff-verbunde (Ph.D. thesis), TU Kaiserslautern; 2015.

[143] Nabovati A, Llewellin EW, Sousa ACM. Through-thickness permeability prediction of three-dimensional multifilament woven fabrics. Compos A: Appl Sci Manuf 2010;41(4):453–63. http://dx.doi.org/10.1016/j.compositesa.2009.11.011.

[144] Bröckel J. Untersuchungen zum einfluss gezielt nicht geradlinig eingebrachter faser-verstärkungen auf die mechanischen eigenschaften einer nachgiebigen polymermatrix (Ph.D. thesis), Universität Rostock; 2007.

[145] Brauner C. Analysis of process-induced distortions and residual stresses of composite structures. Band 8, Logos Verlag Berlin GmbH; 2013.

[146] Gude M, Schirner R, Müller M, Weckend N, Andrich M, Langkamp A. Experimental-numerical test strategy for evaluation of curing simulation of complex-shaped composite structures. Mater Werkst 2016;47(11):1072–86. http://dx.doi.org/10.1002/mawe.201600632.

[147] Andrich A. Analyse des schädigungs- und verformungsverhaltens dickwandiger textilverstärkter kunststoffverbunde bei druckbelastung in dickenrichtung (Ph.D. thesis), Technische Universität Dresden; 2013.

[148] Jakobi R. Zur spannungs-, verformungs- und bruchanalyse an dickwandigen, rohrförmigen bauteilen aus faser-kunststoff-verbunden (Ph.D. thesis), Gesamthochschule Kassel; 1987.

[149] Anandan S, Dhaliwal GS, Huo Z, Chandrashekhara K, Apetre N, Iyyer N. Curing of thick thermoset composite laminates: multiphysics modeling and experiments. Appl Compos Mater 2018;25(5):1155–68. http://dx.doi.org/10.1007/s10443-017-9658-9.

[150] Struzziero G, Skordos AA. Multi-objective optimisation of the cure of thick components. Compos A: Appl Sci Manuf 2017;93:126–36. http://dx.doi.org/10.1016/j.compositesa.2016.11.014.

[151] Dmitriev O, Barsukov A, Dmitriev A. Technological preparation to the manufacturing of thick-walled polymer composite products. 2019.

[152] Balvers JM. In situ strain & cure monitoring in liquid composite moulding by fibre bragg grating sensors (Ph.D. thesis), TU Delft; 2014.

[153] VDI. Entwicklung von bauteilen aus Faser-Kunststoff-Verbund berechnungen. 2006.

[154] Bažant ZP, Planas J. Fracture and size effect in concrete and other quasibrittle materials. Routledge; 2019.

[155] Weibull W. A statistical distribution function of wide applicability. J Appl Mech 1951.

[156] Bažant ZP. Size effect in blunt fracture: Concrete, rock, metal. J Eng Mech 1984;110(4):518–35. http://dx.doi.org/10.1061/(ASCE)0733-9399(1984)110:4(518).

[157] Wisnom MR, Maheri MR. Tensile strength of unidirectional carbon fibre-epoxy from tapered specimens. In: 2nd European conf. on composites testing and standardisation. 1994, p. 239–47.

[158] Wisnom MR. Relationship between strength variability and size effect in unidirectional carbon fibre/epoxy. Composites 1991;22(1):47–52. http://dx.doi.org/10.1016/0010-4361(91)90102-M.

[159] Wisnom MR, Atkinson JW. Reduction in tensile and flexural strength of unidirectional glass fibre-epoxy with increasing specimen size. Compos Struct 1997;38(1–4):405–11. http://dx.doi.org/10.1016/S0263-8223(97)00075-5.

[160] Wisnom MR. The effect of specimen size on the bending strength of unidirectional carbon fibre-epoxy. Compos Struct 1991;18(1):47–63. http://dx.doi.org/10.1016/0263-8223(91)90013-O.

[161] Jackson KE, Tabiei A. Symposium on structural similitude and size effects. In: ASME winter meeting. 1997.

[162] Jackson KE, Kellas S, Morton J. Scale effects in the response and failure of fiber reinforced composite laminates loaded in tension and in flexure. J Compos Mater 1992;26(18):2674–705. http://dx.doi.org/10.1177/002199839202601803.

[163] Jackson KE. Scaling effects in the flexural response and failure of composite beams. AIAA J 1992;30(8):2099–105. http://dx.doi.org/10.2514/3.11186.

[164] Camponeschi ET. Compression testing of thick-section composite materials. In: Composite materials: fatigue and fracture. vol. 3, 1991, p. 439–56.

[165] Camponeschi ET, Gillespie JW, Wilkins DJ. Kink-Band failure analysis of thick composites in compression. J Compos Mater 1993;27(5):471–90. http://dx.doi.org/10.1177/002199839302700502.

[166] Camponeschi ET. Compression response of thick-section composite materials (Ph.D. thesis), University of Delaware; 1990.

[167] Camponeschi ET. Lamina waviness levels in thick composites and its effect on their compression strength. Composites 1991.

[168] Wisnom MR. Size effects in the testing of fibre-composite materials. Compos Sci Technol 1999;59(13):1937–57. http://dx.doi.org/10.1016/S0266-3538(99)00053-6.

[169] Sutherland LS, Shenoi RA, Lewis SM. Size and scale effects in composites: I. Literature review. Compos Sci Technol 1999;59(2):209–20. http://dx.doi.org/10.1016/S0266-3538(98)00065-7.

[170] Zweben C. Size effect in composite materials and structures: Basic concepts and design considerations. In: Scaling effects in composite materials and structures. 1994, p. 197–217.

[171] Bažant ZP. Size effect. Int J Solids Struct 2000;37(1–2):69–80. http://dx.doi.org/10.1016/S0020-7683(99)00077-3.

[172] Soutis C, Curtis PT, Fleck NA. Compressive failure of notched carbon fibre composites. Proc R Soc Lond Ser A: Math Phys Sci 1993;440(1909):241–56. http://dx.doi.org/10.1098/rspa.1993.0014.

[173] Lee J, Soutis C. A study on the compressive strength of thick carbon fibre-epoxy laminates. Compos Sci Technol 2007;67(10):2015–26. http://dx.doi.org/10.1016/j.compscitech.2006.12.001.

[174] Rozylo P. Limit states of thin-walled composite structures with closed sections under axial compression. Compos B: Eng 2024;287:111813. http://dx.doi.org/10.1016/j.compositesb.2024.111813, URL: https://www.sciencedirect.com/science/article/pii/S1359836824006255.

[175] Rozylo P, Debski H. Stability and load carrying capacity of thin-walled composite columns with square cross-section under axial compression. Compos Struct 2024;329:117795. http://dx.doi.org/10.1016/j.compstruct.2023.117795, URL: https://www.sciencedirect.com/science/article/pii/S0263822323011418.

[176] Hodgkinson JM. Mechanical testing of advanced fibre composites. Woodhead Publishing; 2000.

[177] Dogra J, Hodgkinson JM, Robinson P, Pinho ST. Development of a compression test for thick composite laminates: finite element analysis. In: Elastic. vol. 300, 2007, p. 914.

[178] Häberle JG, Matthews FL. An improved technique for compression testing of unidirectional fibre-reinforced plastics; development and results. Composites 1994;25(5):358–71. http://dx.doi.org/10.1016/S0010-4361(94)80006-5.

[179] DIN. Kunststoffe—Bestimmung der zugeigenschaften. Teil 4: Prüfbedingungen für isotrop und anisotrop faserverstärkte kunststoffverbundwerkstoffe. 1997.

[180] DIN. Kunststoffe-bestimmung der zugeigenschaften-teil 5: Prüfbedingungen für unidirektional faserverstärkte kunststoffverbundwerkstoffe. 2010, Deutsche Fassung, Ausgabe Januar.

[181] DIN. Faserverstärkte kunststoffe: Bestimmung der druckeigenschaften in der laminatebene. 2000.

[182] DIN. Faserverstärkte kunststoffe - bestimmung der biegeeigenschaften. 2011.

[183] DIN. Faserverstärkte kunststoffe - zugversuch an 45° -Laminaten zur bestimmung der schubspannungs/schubverformungs-kurve des schubmoduls in der lagenebene. 1998.

[184] Soutis C, Lee J, Kong C. Size effect on compressive strength of T300/924C carbon fibre-epoxy laminates. Plast Rubber Compos 2002;31(8):364–70. http://dx.doi.org/10.1179/146580102225006459.

[185] Gower MR, Shaw RM, Broughton WR. Thick composites: Part I: Mechanical test review, Part II: Cure optimisation. 2008.

[186] Niklewicz J, Sims GD. Size effects in composite materials. 2002.

[187] Lahuerta F, Nijssen RP, van der Meer FP, Sluys LJ. Thickness scaled compression tests in unidirectional glass fibre reinforced composites in static and fatigue loading. Compos Sci Technol 2016;123:115–24. http://dx.doi.org/10.1016/j.compscitech.2015.12.008.

[188] Bažant ZP, Zhou Y, Novák D, Daniel IM. Size effect on flexural strength of fiber-composite laminates. J Eng Mater Technol 2004;126(1):29–37.

[189] Protz R, Kosmann N, Fritsch D, Fey P, Essig W, Dietrich K, Gude M, Horst P, Kreutzbruck M, Schulte K, Busse G, Hufenbach W, Fiedler B. Influence of voids and impact damage on the fatigue behaviour of large scale composites: Einfluss von Poren und Schlagschäden auf das Ermüdungsverhalten von Großstrukturen. Mater Werkst 2016;47(11):1058–71. http://dx.doi.org/10.1002/mawe.201600631.

[190] Johnson DP, Morton J, Kellas S, Jackson KE. Size effects in scaled fiber composites under four-point flexure loading. AIAA J 2000;38(6):1047–54.

[191] Salviato M, Kirane K, Bažant ZP, Cusatis G. Mode I and II interlaminar fracture in laminated composites: A size effect study. J Appl Mech 2019;86(9). http://dx.doi.org/10.1115/1.4043889.

[192] Vassilopoulos A. Fatigue life prediction of composites and composite structures. 2019.

[193] Ganesan R. Fatigue behavior of thick composite laminates. In: Fatigue life prediction of composites and composite structures. Elsevier; 2020, p. 239–67.

[194] Katunin A. Influence of the self-heating effect on fatigue of polymeric laminates. 2012, no. June, S. 24–28.

[195] Lahuerta F. Thickness effect in composite laminates in static and fatigue loading (Ph.D. thesis), TU Delft; 2017.

[196] Hamidi H, Hoa SV, Ganesan R. Material characterization for implementation of hashin tri-axial fatigue failure criteria for unidirectional composite laminates. In: Mechanical behavior of thick composites. 2016.

[197] Feldten D. Beitrag zur steigerung der werkstoffausnutzung von UD-GFK bei biegeschwellbeanspruchung. Shaker; 2014.

[198] Yao L, Rong Q, Shan Z, Qiu Y. Static and bending fatigue properties of ultra-thick 3D orthogonal woven composites. J Compos Mater 2013;47(5):569–77. http://dx.doi.org/10.1177/00219983124431.

[199] Hosoi A, Sakuma S, Seki S, Fujita Y, Taketa I, Kawada H. Effect of stress ratio on fatigue characteristics in the out-of-plane direction of thick CFRP laminates with toughened interlaminar layers. In: Proceedings of the 20th international conference on composite materials. 2015, URL: http://iccm20.org/fullpapers/file.

[200] Hansen JZ, Østergaard R. The effects of fibre architecture on fatigue life-time of composite materials. 2013.

[201] Draskovic M, Galappathithi UI, Pickett AK, Capellaro M, Middendorf P. Influence of ply waviness on residual strength and fatigue degradation of composite wind turbine blades. In: ICCM19.

[202] Chou PC, Croman R. Scale effect in fatigue of composite materials. J Compos Mater 1979;13(3):178–94. http://dx.doi.org/10.1177/002199837901300 3.

[203] Crowther MF, Starkey MS. Use of Weibull statistics to quantify specimen size effects in fatigue of GRP. Compos Sci Technol 1988;31(2):87–95. http://dx.doi.org/10.1016/0266-3538(88)90084-X.

[204] Tai NH, Ma CC, Lin JM, Wu GY. Effects of thickness on the fatigue-behavior of quasi-isotropic carbon/epoxy composites before and after low energy impacts. Compos Sci Technol 1999;59(11):1753–62. http://dx.doi.org/10.1016/S0266-3538(99)00037-8.

[205] Mirzaei AH, Shokrieh MM. Simulation and measurement of the self-heating phenomenon of carbon/epoxy laminated composites under fatigue loading. Compos B: Eng 2021;(223). http://dx.doi.org/10.1016/j.compositesb.2021.109097.

[206] van Wingerde A. Evaluation on the effect of thick laminates wp10. 2006.

[207] Liu H, Ojha A, Li Z, Engler-Pinto Jr. CC, Su X, Sun Q, Kang H, Wen W, Cui H. Fatigue modeling for carbon/epoxy unidirectional composites under various stress ratios considering size effects. Int J Fatigue 2019;120:184–200. http://dx.doi.org/10.1016/j.ijfatigue.2018.11.009.

[208] Lahuerta F, Westphal T, Nijssen RP. Self-heating forecasting for thick laminates testing coupons in fatigue. In: The science of making torque from wind. Torque; 2012.

[209] Katunin A. Criticality of the self-heating effect in polymers and polymer matrix composites during fatigue, and their application in non-destructive testing. Polymers 2018;11(1):19. http://dx.doi.org/10.3390/polym11010019.

[210] Lahuerta F, Westphal T, Nijssen RP, van der Meer FP, Sluys LJ. Static and fatigue performance of thick laminates test design and experimental compression results. In: ECCM-16th. 2014.

[211] Lahuerta F, Nijssen RP, van der Meer FP, Sluys LJ. Experimental-computational study towards heat generation in thick laminates under fatigue loading. Int J Fatigue 2015;80:121–7.

[212] Lahuerta F. Thickness scaled compression tests in unidirectional glass fibre reinforced composites in static and fatigue loading. Compos Sci Technol 2016;123:115–24. http://dx.doi.org/10.1016/j.compscitech.2015.12.008.

[213] Heimbs S. Foldcore sandwich structures and their impact behaviour: An overview. In: Dynamic failure of composite and sandwich structures. Springer Netherlands; 2012, p. 491–544.

[214] Evci C. Thickness-dependent energy dissipation characteristics of laminated composites subjected to low velocity impact. Compos Struct 2015;133:508–21. http://dx.doi.org/10.1016/j.compstruct.2015.07.111.

[215] Islam F, Caldwell R, Phillips AW, St John NA, Prusty BG. A review of relevant impact behaviour for improved durability of marine composite propellers. Compos C: Open Access 2022;8:100251. http://dx.doi.org/10.1016/j.jcomc.2022.100251.

[216] Pinnell M, Sjoblom P. Low-Velocity impact testing of thermoplastic and thermoset matrix composite materials. 1990.

[217] de Morais WA, Monteiro SN, d'Almeida JRM. Effect of the laminate thickness on the composite strength to repeated low energy impacts. Compos Struct 2005;70(2):223–8. http://dx.doi.org/10.1016/j.compstruct.2004.08.024.

[218] Atas C, Icten BM, Küçük M. Thickness effect on repeated impact response of woven fabric composite plates. Compos B: Eng 2013;49:80–5. http://dx.doi.org/10.1016/j.compositesb.2013.01.019.

[219] Belingardi G, Vadori R. Influence of the laminate thickness in low velocity impact behavior of composite material plate. Compos Struct 2003;61(1–2):27–38. http://dx.doi.org/10.1016/s0263-8223(03)00027-8.

[220] Guynn E, Obrien T. The influence of lay-up and thickness on composite impact damage and compression strength. In: 26th structures, structural dynamics, and materials conference. American Institute of Aeronautics and Astronautics; 1985.

[221] Duan M, Yue Z, Song Q. Investigation of damage to thick composite laminates under low-velocity impact and frequency-sweep vibration loading conditions. Adv Mech Eng 2020;12(10):168781402096504. http://dx.doi.org/10.1177/1687814020965042.

[222] Reis P, Sousa P, Ferreira LM, Coelho C. Multi-impact response of semicylindrical composite laminated shells with different thicknesses. Compos Struct 2023;310:116771. http://dx.doi.org/10.1016/j.compstruct.2023.116771, URL: https://www.sciencedirect.com/science/article/pii/S0263822323001150.

[223] Breen C, Guild F, Pavier M. Impact damage to thick carbon fibre reinforced plastic composite laminates. J Mater Sci 2006;41(20):6718–24. http://dx.doi.org/10.1007/s10853-006-0208-3.

[224] Yang FJ, Cantwell WJ. Impact damage initiation in composite materials. Compos Sci Technol 2010;70(2):336–42. http://dx.doi.org/10.1016/j.compscitech.2009.11.004.

[225] Agrawal S, Singh KK, Sarkar PK. Impact damage on fibre-reinforced polymer matrix composite – A review. J Compos Mater 2013;48(3):317–32. http://dx.doi.org/10.1177/0021998312472217.

[226] Aoki Y, Samejima H, Suemasu H, Nagao Y. Effect of thickness on impact damage and CAI behavior. In: Proceedings of ICCM-17 17th international conference on composite materials. 2009.

[227] Schoeppner GA, Abrate S. Delamination threshold loads for low velocity impact on composite laminates. Compos A: Appl Sci Manuf 2000;31(9):903–15. http://dx.doi.org/10.1016/s1359-835x(00)00061-0.

[228] Aoki Y, Samejima H, Suemasu H, Nagao Y. Effect of thickness on impact damage and CAI behavior. In: ICCM international conferences on composite materials. 2009.

[229] Riegert G, Keilig T, Aoki R, Drechsler K, Busse G. Schädigungscharakterisierung an NCF-laminaten mittels lockin-thermographie und bestimmung der CAI-restfestigkeiten. In: (Hrsg.) C, editor. Eisenbach. vol. 19, 2005.

[230] Abir M, Tay T, Ridha M, Lee H. On the relationship between failure mechanism and compression after impact (CAI) strength in composites. Compos Struct 2017;182:242–50. http://dx.doi.org/10.1016/j.compstruct.2017.09.038, URL: https://www.sciencedirect.com/science/article/pii/S026382231732384X.

[231] Lin S, Ranatunga V, Waas AM. Experimental study on the panel size effects of the low velocity impact (LVI) and compression after impact (CAI) of laminated composites, part II: CAI. Compos Struct 2022;295:115824. http://dx.doi.org/10.1016/j.compstruct.2022.115824, URL: https://www.sciencedirect.com/science/article/pii/S0263822322005943.

[232] Caminero M, García-Moreno I, Rodríguez G. Experimental study of the influence of thickness and ply-stacking sequence on the compression after impact strength of carbon fibre reinforced epoxy laminates. Polym Test 2018;66:360–70. http://dx.doi.org/10.1016/j.polymertesting.2018.02.009, URL: https://www.sciencedirect.com/science/article/pii/S0142941817319219.

[233] Liu D, Raju B, Dang X. Size effects on impact response of composite laminates. Int J Impact Eng 1998;21(10):837–54. http://dx.doi.org/10.1016/s0734-743x(98)00036-0.

[234] Safri S, Sultan M, Yidris N, Mustapha F. Low velocity and high velocity impact test on composite materials - A review. Int J Eng Sci 2014;3:50–60.

[235] Nguyen LH, Ryan S, Cimpoeru SJ, Mouritz AP, Orifici AC. The effect of target thickness on the ballistic performance of ultra high molecular weight polyethylene composite. Int J Impact Eng 2015;75:174–83.

[236] Siva Kumar K, Balakrishna Bhat T. Response of composite laminates on impact of high velocity projectiles. In: Key engineering materials. vol. 141, 1998, p. 337–48.

[237] Sikarwar RS, Velmurugan R, Madhu V. Experimental and analytical study of high velocity impact on Kevlar/Epoxy composite plates. Cent Eur J Eng 2012;2(4):638–49.

[238] Gellert EP, Cimpoeru SJ, Woodward RL. A study of the effect of target thickness on the ballistic perforation of glass-fibre-reinforced plastic composites. Int J Impact Eng 2000;24(5):445–56.

[239] Hosur MV, Vaidya UK, Ulven C, Jeelani S. Performance of stitched/unstitched woven carbon/epoxy composites under high velocity impact loading. Compos Struct 2004;64(3–4):455–66.

[240] Gunes R, Al-Behadili DS. Damage behaviors of thin and thick laminated composites under ballistic effect. Mech Compos Mater 2024;60(2):243–58. http://dx.doi.org/10.1007/s11029-024-10187-1.

[241] Zhang D, Sun Y, Chen L, Zhang S, Pan N. Influence of fabric structure and thickness on the ballistic impact behavior of Ultrahigh molecular weight polyethylene composite laminate. Mater Des (1980-2015) 2014;54:315–22. http://dx.doi.org/10.1016/j.matdes.2013.08.074.
[242] Zhao S, Huang J, Cao J, Chen Y, Zuo X, Yi K, Zhang C. Thickness effect on ballistic impact behavior of hybrid carbon/Kevlar composites. Compos Sci Technol 2024;254:110692. http://dx.doi.org/10.1016/j.compscitech.2024.110692.
[243] Daum B, Feld N, Allix O, Rolfes R. A review of computational modelling approaches to compressive failure in laminates. Compos Sci Technol 2019;181:107663. http://dx.doi.org/10.1016/j.compscitech.2019.05.020, URL: https://www.sciencedirect.com/science/article/pii/S0266353818329063.
[244] Daum B, Gottlieb G, Safdar N, Brod M, Ohlendorf J-H, Rolfes R. A numerical investigation of the statistical size effect in non-crimp fabric laminates under homogeneous compressive loads. J Compos Mater 2022;56(5):665–83. http://dx.doi.org/10.1177/00219983211057346, arXiv:https://doi.org/10.1177/00219983211057346.
[245] Kuhlmann G, Rolfes R. A hierarchic 3D finite element for laminated composites. Internat J Numer Methods Engrg 2004;61(1):96–116. http://dx.doi.org/10.1002/nme.1060.
[246] Scheider I, Chen Y, Hinz A, Huber N, Mosler J. Size effects in short fibre reinforced composites. Eng Fract Mech 2013;100:17–27. http://dx.doi.org/10.1016/j.engfracmech.2012.05.005, URL: https://www.sciencedirect.com/science/article/pii/S0013794412002007, Crack growth in brittle materials.
[247] Salviato M, Kirane K, Esna Ashari S, Bažant ZP, Cusatis G. Experimental and numerical investigation of intra-laminar energy dissipation and size effect in two-dimensional textile composites. Compos Sci Technol 2016;135:67–75. http://dx.doi.org/10.1016/j.compscitech.2016.08.021, URL: https://www.sciencedirect.com/science/article/pii/S0266353816303384.
[248] Li X, Hallett SR, Wisnom MR. A finite element based statistical model for progressive tensile fibre failure in composite laminates. Compos B: Eng 2013;45(1):433–9.
[249] Okabe T, Takeda N. Size effect on tensile strength of unidirectional CFRP composites—experiment and simulation. Compos Sci Technol 2002;62(15):2053–64.
[250] Varandas LF, Catalanotti G, Melro AR, Falzon BG. On the importance of nesting considerations for accurate computational damage modelling in 2D woven composite materials. Comput Mater Sci 2020;172:109323.
[251] Düreth C, Weck D, Böhm R, Thieme M, Gude M, Wolf CH, Henkel S, Biermann H. Interlaminar shear strength enhancement under out-of-plane compression of fabric reinforcements - a review on meso and macro scale. In: Proceedings of the 18th European conference on composite materials. Athen, Greece; 2018, p. 10.
[252] Düreth C, Weck D, Böhm R, Thieme M, Gude M, Henkel S, Wolf CH, Biermann H. Determining the Damage and Failure Behaviour of Textile Reinforced Composites under Combined In-Plane and Out-of-Plane Loading. Materials 2020;13(21):4772. http://dx.doi.org/10.3390/ma13214772.
[253] Wolf CH, Henkel S, Düreth C, Gude M, Biermann H. Characterization of the fatigue crack growth behavior of fabric-reinforced fiber-plastic composites under interlaminar shear and out-of-plane compressive loading. Procedia Struct Integr 2024;66:26–37. http://dx.doi.org/10.1016/j.prostr.2024.11.052, URL: https://linkinghub.elsevier.com/retrieve/pii/S2452321624011004.
[254] Wang B, Zhong S, Lee T-L, Fancey KS, Mi J. Non-destructive testing and evaluation of composite materials/structures: A state-of-the-art review. Adv Mech Eng 2020;12(4):168781402091376. http://dx.doi.org/10.1177/1687814020913761.
[255] Gholizadeh S. A review of non-destructive testing methods of composite materials. Procedia Struct Integr 2016;1:50–7. http://dx.doi.org/10.1016/j.prostr.2016.02.008.
[256] Amafabia DM, Montalvão D, David-West O, Haritos G. A review of structural health monitoring techniques as applied to composite structure. Struct Durab Heal Monit 2017;(11):91–147.
[257] Solodov I, Bernhardt Y, Littner L, Kreutzbruck M. Ultrasonic anisotropy in composites: Effects and applications. J Compos Sci 2022;6(3):93–115. http://dx.doi.org/10.3390/jcs6030093.
[258] Teti R, Caprino G. NDE of thick GFRP composites through ultrasonic waveform detection. In: Bunsell AR, Lamicq P, Massiah A, editors. Developments in the science and technology of composite materials. Springer; 1989, p. 793–800.
[259] Bunsell AR, Lamicq P, Massiah A. Developments in the science and technology of composite materials. Springer; 1989.
[260] Rao BPC. Non-destructive testing and damage detection. In: Prasad NE, Wanhill R, editors. Aerospace materials and material technologies (Indian institute of metals series). Springer; 2017, p. 209–28.
[261] Quinn J, Patsia O, Giannopoulos A, Brádaigh C, McCarthy E. Novel application of ground penetrating radar for damage detection in thick FRP composites. Compos B: Eng 2024;284(111716). http://dx.doi.org/10.1016/j.compositesb.2024.111716.
[262] Kim D, Ryu C, Park S, Kim S. Nondestructive evaluation of hidden damages in glass fiber reinforced plastic by using the terahertz spectroscopy. Int J Precis Eng Manuf-Green Technol 2017;4:2011–9. http://dx.doi.org/10.1007/s40684-017-0026-x.
[263] Tao N, Anisimov A, Groves R. Shearography non-destructive testing of thick GFRP laminates: Numerical and experimental study on defect detection with thermal loading. Compos Struct 2022;282(115008). http://dx.doi.org/10.1016/j.compstruct.2021.115008.
[264] Borum K. Evaluation of the quality of thick fibre composites using immersion and air-coupled ultrasonic techniques. In: 9th European conference on NDT. 2006.
[265] Teller CM, Fortunko CM. NDE requirements for thick marine composites. In: Thompson DO, Chimenti DE, editors. Review of progress in quantitative nondestructive evaluation. Springer US; 1991, p. 1599–606.
[266] Scarponi C, Briotti G. Ultrasonic technique for the evaluation of delaminations on CFRP, GFRP, KFRP composite materials. Compos B: Eng 2000;31(3):237–43. http://dx.doi.org/10.1016/S1359-8368(99)00076-1.
[267] Hawkins GF, Sheaffer PM, Johnson EC. NDE of thick composites in the aerospace industry — An overview. In: Thompson DO, Chimenti DE, editors. Review of progress in quantitative nondestructive evaluation. Springer US; 1991, p. 1591–7.
[268] Roberts RA. Porosity characterization in fiber-reinforced composites by use of ultrasonic backscatter. In: Thompson DO, Chimenti DE, editors. Review of progress in quantitative nondestructive evaluation. Springer US; 1987, p. 1147–56.
[269] Mouritz AP, Townsend C, Shah Khan MZ. Non-destructive detection of fatigue damage in thick composites by pulse-echo ultrasonics. Compos Sci Technol 2000;60(1):23–32. http://dx.doi.org/10.1016/S0266-3538(99)00094-9.
[270] Solodov I, Döring D, Rheinfurth M, Busse G. Ultrasonic NDT of in-plane stiffness anisotropy in metals and composites. In: 10th European conference on non-destructive testing. 2010.
[271] Thalapil J, Sawant S, Tallur S, Banerjee S. Guided wave based localization and severity assessment of in-plane and out-of-plane fiber waviness in carbon fiber reinforced composites. Compos Struct 2022;297:115932. http://dx.doi.org/10.1016/j.compstruct.2022.115932.
[272] Zhang Z, Cao A, Li Q, Yang W, Li Y. Imaging of fiber waviness in thick composites with unknown material properties using probability-based ultrasound non-reciprocity. Materials 2023;16(10). http://dx.doi.org/10.3390/ma16103786.
[273] Li C, Pain D, Wilcox PD, Drinkwater BW. Imaging composite material using ultrasonic arrays. NDT E Int 2013;53:8–17. http://dx.doi.org/10.1016/j.ndteint.2012.07.006.
[274] Fortunko CM, Fitting DW. Apropriate ultrasonic system components for NDE of thick Polymer-Composites. In: Thompson DO, Chimenti DE, editors. Review of progress in quantitative nondestructive evaluation. Springer US; 1991, p. 2105–12.
[275] Hsu DK. Inspecting composites with airborne ultrasound: Through thick and thin. In: AIP conference proceedings. p. 991–8. http://dx.doi.org/10.1063/1.2184633, 200.
[276] Vopálenský M, Vavřík D, Kumpová I. Optimization of the X-ray tube voltage with respect to the dynamical resolution in radiography and tomography. In: 8th conference on industrial computed tomography. 2018.
[277] Sket F, Enfedaque A, Alton C, González C, Molina-Aldareguia J, Llorca J. Automatic quantification of matrix cracking and fiber rotation by X-ray computed tomography in shear-deformed carbon fiber-reinforced laminates. Compos Sci Technol 2014;90:129–38. http://dx.doi.org/10.1016/j.compscitech.2013.10.022, URL: https://www.sciencedirect.com/science/article/pii/S0266353813004223.
[278] Highsmith AL. Post-impact behavior of composite solid rocket motor cases. In: 1992 NASA (ASEE summer faculty fellowship program). Alabama Univ.; 1992.
[279] Tan KT, Watanabe N, Iwahori Y. X-ray radiography and micro-computed tomography examination of damage characteristics in stitched composites subjected to impact loading. Compos B: Eng 2011;42(4):874–84. http://dx.doi.org/10.1016/j.compositesb.2011.01.011.
[280] Soutis C, Fleck N, Smith P. Compression fatigue behaviour of notched carbon fibre-epoxy laminates. Int J Fatigue 1991;13(4):303–12.
[281] Commission UNR. Introduction to liquid penetrant examination. 2008, URL: https://www.nrc.gov/docs/ML1214/ML12146A180.pdf. [Zugriff 19 August 2025].
[282] Djukic LP, Herszberg I, Walsh WR, Schoeppner GA, Gangadhara Prusty B. Contrast enhancement in visualisation of woven composite architecture using a MicroCT Scanner. Part 2: Tow and preform coatings. Compos A: Appl Sci Manuf 2009;40(12):1870–9. http://dx.doi.org/10.1016/j.compositesa.2009.04.002, URL: https://www.sciencedirect.com/science/article/pii/S1359835X09000839, Special Issue: CompTest 2008.
[283] Goossens E, De Baere I, Sinchuk Y, Dhaene E, De Vos J, Rooms P, Boone MN, De Roo J, Van Driessche I, Van Paepegem W, et al. Contrast-enhanced imaging of carbon fiber composites using hafnium oxide nanocrystals. Nanoscale 2025;17(16):10219–38.
[284] Weight K. An overview of NDE methods for thick composites and a proposal for analysis of computed technology data. 1994, Online: https://apps.dtic.mil/sti/citations/ada288733.
[285] Kastner J, Plank B, Salaberger D, Sekelja J. Defect and porosity determination of fibre reinforced polymers by X-ray computed tomography. In: 2nd international symposium on NDT in aerospace. 2010.

[286] Emerson MJ, Jespersen KM, Dahl AB, Conradsen K, Mikkelsen LP. Individual fibre segmentation from 3D X-ray computed tomography for characterising the fibre orientation in unidirectional composite materials. Compos A: Appl Sci Manuf 2017;97:83–92. http://dx.doi.org/10.1016/j.compositesa.2016.12.028.

[287] Garcea SC, Wang Y, Withers PJ. X-ray computed tomography of polymer composites. Compos Sci Technol 2018;156:305–19. http://dx.doi.org/10.1016/j.compscitech.2017.10.023.

[288] Bull DJ, Helfen L, Sinclair I, Spearing SM, Baumbach T. A comparison of multi-scale 3D X-ray tomographic inspection techniques for assessing carbon fibre composite impact damage. Compos Sci Technol 2013;75:55–61. http://dx.doi.org/10.1016/j.compscitech.2012.12.006.

[289] Myrach P, Maierhofer C, Rahammer M, Kreutzbruck M. Parameters in lock-in thermography of CFRP laminates. Mater Test 2016;58(1):31–5. http://dx.doi.org/10.3139/120.110814.

[290] Li T, Almond DP, Rees DAS. Crack imaging by scanning laser-line thermography and laser-spot thermography. Meas Sci Technol 2011;22(3):35701. http://dx.doi.org/10.1088/0957-0233/22/3/035701.

[291] Solodov I, Rahammer M, Busse G. A local defect resonance for linear and nonlinear ultrasonic thermography. In: Proceedings of the 2012 international conference on quantitative infraRed thermography. 2012, http://dx.doi.org/10.21611/qirt.2012.385.

[292] Vavilov V. Determining limits of thermal NDT of thick Graphite/Epoxy composites. In: 9th European conference on NDT. 2006.

[293] Jolly MR, Prabhakar A, Sturzu B, Hollstein K, Singh R, Thomas S, Foote P, Shaw A. Review of non-destructive testing (NDT) techniques and their applicability to thick walled composites. Procedia CIRP 2015;38:129–36.

[294] Worzewski T, Krankenhagen R, Doroshtnasir M, Röllig M, Maierhofer C, Steinfurth H. Thermographic inspection of a wind turbine rotor blade segment utilizing natural conditions as excitation source, Part I: Solar excitation for detecting deep structures in GFRP. Infrared Phys Technol 2016;76:756–66. http://dx.doi.org/10.1016/j.infrared.2016.04.011.

[295] Reocreux L, Yu Z, Arnould S, Pron H. Passive thermography for delamination detection in GFRP of Wind Turbine Blade. In: Proceedings of the 2020 international conference on quantitative infraRed thermography. 2020, http://dx.doi.org/10.21611/qirt.2020.036.

[296] Burgholzer P, Mayr G, Gruber J, Stockner G. Thermografische rekonstruktion von internen Wärmequellen mittels virtueller Schallwellen. Mater Test 2018;60(6):600–6. http://dx.doi.org/10.3139/120.111192.

[297] Rittmann J, Kreutzbruck M. 3D-thermografie mittels künstlicher intelligenz. In: DGZfP jahrestagung 2022. 2022.

[298] Holtmann N. Auswertung und anregung eindimensionalen wärmeflusses in der zerstörungsfreien bauteilprüfung mittels optisch angeregter lockin-thermografie (Ph.D. thesis), Universität Stuttgart; 2015.

[299] Rittmann J, Kreutzbruck M. Lateral heat flux reduction using a lock-in thermography compensation method. Sci Rep 2023;13(17093). http://dx.doi.org/10.1038/s41598-023-44128-0.

[300] Sause MGR, Horn S. Quantification of the uncertainty of pattern recognition approaches applied to acoustic emission signals. J Nondestruct Eval 2013;32(3):242–55. http://dx.doi.org/10.1007/s10921-013-0177-9.

[301] Kelke B. On the influence of source depth and source-to-sensor distance on the acoustic emission signatures of damaging events in cross-ply carbon fibre-reinforced plastics (Ph.D. thesis), Technische Universität Kaiserslautern; 2020.

[302] Tang J, Soua S, Mares C, Gan T-H. An experimental study of acoustic emission methodology for in service condition monitoring of wind turbine blades. Renew Energy 2016;99:170–9. http://dx.doi.org/10.1016/j.renene.2016.06.048.

[303] Doliński Ł, Krawczuk M, Żak A. Damage detection in the wind turbine blade using root mean square and experimental modal parameters. In: Wahab M, editor. Proceedings of the 13th international conference on damage assessment of structures. Springer; 2020, p. 728–42.

[304] Poozesh P, Aizawa K, Niezrecki C, Baqersad J, Inalpolat M, Heilmann G. Structural health monitoring of wind turbine blades using acoustic microphone array. Struct Heal Monit 2017;16(4):471–85. http://dx.doi.org/10.1177/1475921716676871.